Testing and Demonstration of Remote and Autonomous Control Architecture for the Very-Small, Long-Life, Modular (VSLLIM) Microreactor

Mohamed S. El-Genk, Timothy Schriener
Institute for Space and Nuclear Power Studies and Nuclear Engineering Department, The University of New Mexico, Albuquerque, NM, USA

Technical Work Scope: *Nuclear Energy– Innovative Microreactor Solutions for End-User Applications (RC-2).* DOE-NEUP Project 22-26910. DOE Office of Nuclear Energy's Nuclear Energy University Programs award through a subaward from Purdue University to the University of New Mexico's Institute for Space and Nuclear Power Studies under contract DE-NE0009268

Report No. UNM-ISNPS-01-2026
Institute for Space and Nuclear Power Studies, The University of New Mexico, Albuquerque, NM, USA, http://isnps.unm.edu/reports/

January 2026

Abstract

This report details the work conducted by the research team at the University of New Mexico's Institute for Space and Nuclear Power Studies (UNM-ISNPS) on Demonstrating Autonomous Control, Remote Operation, and Human Factors for Microreactors. The effort for *Task 2 - Testing and Demonstration* focused on the development, testing, and demonstration of the remote and autonomous control system using trained Artificial Neural Networks (ANN) for control of the developed digital twin of the Very-Small, Long-LIfe, Modular (VSLLIM) microreactor. This walk-away safe reactor can continuously generate 1.0 - 10 MW of thermal power for 92 and 5.6 full power years, respectively, is cooled by natural circulation of in-vessel liquid sodium. The task trained Reinforcement Learning (RL) Soft Actor Critic algorithms with Feedforward Neural Network (SAC-FNN) to control the position of the control rods in the reactor core of the VSLLIM digital twin during simulated startup transients. The trained SAC-FNN algorithms successfully completed the startup scenario, accurately predicting the control rods positions to within ±1.6% of the target values. The trained neural networks are incorporated into a Programmable Logic Controller (PLC) for real-time control of the VSLLIM's digital twin model. The PLC with trained SAC-FNN algorithms showed satisfactory performance, regulating the withdrawal of the control rods to ensure a smooth rise in the reactor power and sodium temperatures. It also determined the control rod positions within ±0.7% of the target values. The performance of the trained SAC-FNN algorithms is superior to that demonstrated by the Supervised Learning algorithms in Task 1 of this project. The PLC with trained SAC-FNN algorithms is integrated into a testbed developed to demonstrate the remote operation and control the VSLLIM microreactor. This testbed, located in a separate building remote from the building housing the reactor digital twin model, uses a two-step encryption scheme. It secures the communication and data exchange between the digital control system of the reactor and the remote human operator. The developed operator terminal software with a Graphical User Interface (GUI) provides real-time monitoring of the remote reactor and plotting of the plant operational variables and sends commands to the PLC to implement. Testing of the platform examines different transient scenarios including commanding changes in the reactor power level by the PLC with SAC-FNN algorithms to different operator specified setpoints. A performed demonstration of the remote-control testbed had student researchers at Purdue University successfully control the startup of the VSLLIM digital twin at UNM-ISNPS.

List of Contents

List of Figures

List of Tables

Nomenclature

AES	Advanced Encryption Standard
b	neurons biases
CRP	Control Rod Position
CRP*	Normalized Control Rod Position
ESD	Emergency Shut Down
F	Feature of State Variables Array
F*	Normalized Feature of State Variables Array
FNN	Feed-forward Neural Network
FPY	Full Power Years
HEX	Heat Exchanger
I&C	Instrumentation and Control
LMHP-TE	Liquid Metal Heat Pipe-Thermoelectric auxiliary power generation modules
LOBO NCS	LOBO Nuclear CyberSecurity
LSTM	Long Short-Term Memory
$\dot{m}$	Mass flow rate (kg/s)
ML	Machine Learning
MMR	Modular Microreactor
Na	Liquid sodium
NIST	National Institute of Standards and Technology
P_{Rx}	Reactor Thermal Power (kW, MW)
P_{sp}	Power setpoint (MW_{th})
PD	Proportional-Differential
PI	Proportional-Integral
PID	Proportional-Integral-Differential
PLC	Programmable Logic Controller
RC	Reactor Control
RL	Reinforcement Learning
RSA	Rivest–Shamir–Adleman
SAC	Soft Actor Critic
SAC-FNN	Soft Actor Critic algorithm with Feed-forward Neural Network
SL	Supervised Learning
SL-LSTM	Supervised Learning algorithm with Long Short-Term Memory network
T_{in}	Sodium coolant inlet temperature (K)
T_{ex}	Sodium outlet temperature (K)
T_{in}^{Rx}	Reactor core inlet temperature (K)
TLS	Transport Layer Security
UNM-ISNPS	University of New Mexico's Institute for Space and Nuclear Power Studies
VSLLIM	**V**ery-**S**mall, **L**ong-**LI**fe, Modular
Y	Output value
w	Neurons weights
X	Feature value
X*	Normalized feature value
X_{max}	Feature highest value.

X_{min}	Feature lowest value.

Greeks

α	Controller scaling coefficient, Activation function
$\Delta\rho$	Reactivity insertion / feedback ($)
λ_e	Effective constant for a delayed neutron group (s^{-1})
μ	Actor network mean
ρ	Total reactivity ($) or PCM
σ	Actor network standard deviation
τ	Reactor period, burnup (MWd)

Subscripts and Superscripts

0	Initial state
b	Bulk
BeO	Beryllium Oxide
Bu	Burnup
CR	Control Rod
Dop	Doppler effect
ex	External
fb	Feedback
fuel	nuclear fuel.
g	Generated state
HEX	Na/Na heat exchanger.
Na	Liquid sodium
Rx	Reactor
SP	Setpoint

1. Introduction

The digital Instrumentation and Control (I&C) systems of modular small and micro reactors at remote sites would send monitoring information to the human operator in the control center who in return sends commands to start up and shut down the reactors or change their operating power levels [Agarwal, Ballout, and Gehin 2021]. Such an arrangement could allow a single team of human operators to control multiple micro-reactor units located at remote locations from the control center (Fig. 1). Safe, remote control will also require securing communications against outside actors attempting to send false commands or monitoring signals or record the plant operation state data to aid in planning cyberattacks. Such systems must also be capable of local autonomous, fail-safe operation if communication lines between the plant and remote operator are blocked or severed.

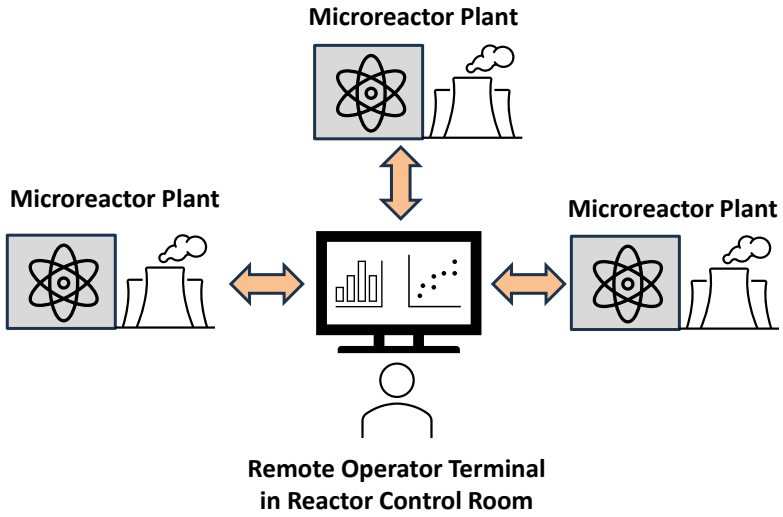

Fig. 1. A block diagram of a human operator in the control room monitoring multiple microreactor units at remote sites.

Training and implementing Machine Learning (ML) algorithms can enable fail-safe operation and autonomous control of these reactors. These algorithms are trained from operation data to learn to produce generalized responses to perform tasks without explicit instructions. They would monitor and diagnose anomalous operating conditions, independently take corrective control actions [Cetiner 2016] and monitor sensor data as well as detect, identify, and correct faults [Tang 2022].

1.1 Objectives

The objectives of this task at UNM-ISNPS are to develop and demonstrate remote and autonomous control of the Very-Small, Long-LIfe, Modular (VSLLIM) microreactor developed at UNM-ISNPS [El-Genk and Palomino 2019; El-Genk, Schriener, and Palomino 2021]. The research investigates training ML algorithms for autonomous control of the VSLLIM microreactor. In Task 1 our research team investigated training Supervised Learning (SL) algorithms for reactor control of the VSLLIM microreactor [El-Genk, Schriener, and Shaheen 2024]. Results showed that although the predictions of the SL algorithms are highly accurate, they had inferior performance when incorporated into a Programmable Logic Controller (PLC) and applied to real-time control of a digital twin model of the VSLLIM

microreactor excluded them from further consideration. The research effort in Task 2 therefore focuses on training Reinforcement Learning (RL) algorithms while coupled directly to the VSLLIM microreactor digital twin [El-Genk, Schriener, and Shaheen 2025]. RL algorithms train agents to receive a high cumulative reward for making correct actions while actively controlling a dynamic process [Sutton 2018]. Training RL algorithms seeks balance between exploring the action space and exploiting the current knowledge of the controller's responses [Sutton 2018; Kaelbling, Littman, and Moore 1996]. This feature allows RL algorithms to examine different control actions and identify the most advantageous response.

This research trains RL Soft-Actor Critic algorithms with Feedforward Neural Networks (SAC-FNN) to manage the movement of the control rods in the core of the VSLLIM microreactor [El-Genk and Palomino 2019; El-Genk, Schriener, and Palomino 2021] during simulated startup transients to steady thermal power levels of 1.0 – 10 MW_{th}. The SAC-FNN algorithm which has early shown superior performance in control processes [Lee, et al. 2021; Bae, Kim, Lee 2023] uses an Actor network for making control decisions and a Critic network for judging the performance of the Actor network. It also updates the weights and biases during training and the Actor and Critic networks using data throughout the entire transient to prevent local overfitting of the weights and the biases of the neural networks [Sutton 2018; Bae, Kim, Lee 2023]. The trained SAC-FNN algorithms are evaluated while integrated into a software PLC to evaluate and compare their performance for real-time control of the VSLLIM microreactor during the same simulated startup transients. Results examine the differences in the responses of the PLC with trained SAC-FNN algorithms compared with the SL algorithms in Task 1.

The PLC with trained SAC-FNN networks is then integrated within a developed secure, remote-control testbed incorporating a digital twin model of the VSLLIM microreactor developed using MATLAB Simulink software [El-Genk, Schriener, and Shaheen 2025]. The human operator has a virtual console that displays the operation variables generated by the VSLLIM digital twin on a large format screen using a Graphical User Interface (GUI) application. The operator monitors the operation state of the simulated reactor and sends commands to change the reactor operation. The developed remote-control platform secures communication between the remote operator terminal and the controllers of the VSLLIM reactor using two levels of data encryption. Testing for the developed remote-control testbed with PLC incorporating the trained SAC-FNNs algorithms evaluates its performance for controlling the VSLLIM digital twin model for a range of operation transients, including startup and changes in reactor power. The testbed is then demonstrated by allowing researchers at Purdue University to control the startup of the VSLLIM digital twin at UNM-ISNPS. The following section briefly describes the design features and control of the VSLLIM microreactor.

2. VSLLIM Microreactor Design Features and Control

The performed training of the SAC-FNN algorithms used a developed MATLAB-Simulink VSLLIM microreactor digital twin for simulated startup transients to steady power levels of 1.0 – 10 MW_{th}. The fast spectrum, walk-away safe VSLLIM microreactor operates fully passively and (Figs. 2, 3) is cooled by natural circulation of in-vessel liquid sodium (Na) during nominal operation and after shutdown. This is aided by a 2-m tall chimney and a helically coiled-tubes Na/Na heat exchanger (HEX) placed at the top entrance to the downcomer (Figs. 2, 3) [El-Genk and Palomino 2019; El-Genk, Schriener, and Palomino 2021]. The VSLLIM reactor design offers redundant control and passive removal of decay heat after shutdown and employes liquid metal heat-pipe thermoelectric (LMHP-TE) conversion modules cooled by

natural convection of ambient air. They generate auxiliary DC power 24/7 during reactor operation and after shutdown, and in case of an unlikely loss of both off-site and on-site power sources. This factory fabricated, assembled, and sealed modular microreactor can continuously generate 1.0 MW of thermal power for 92 full power years and up to 10.0 MW for ~5.9 Years (FPY), without refueling [El-Genk and Palomino 2019]. It arrives at the operating site on an 18-wheeler truck, by rail, or on a barge and is mounted underground on seismic isolation bearings to protect against earthquakes and an airplane crash or a missile impact (Fig. 3).

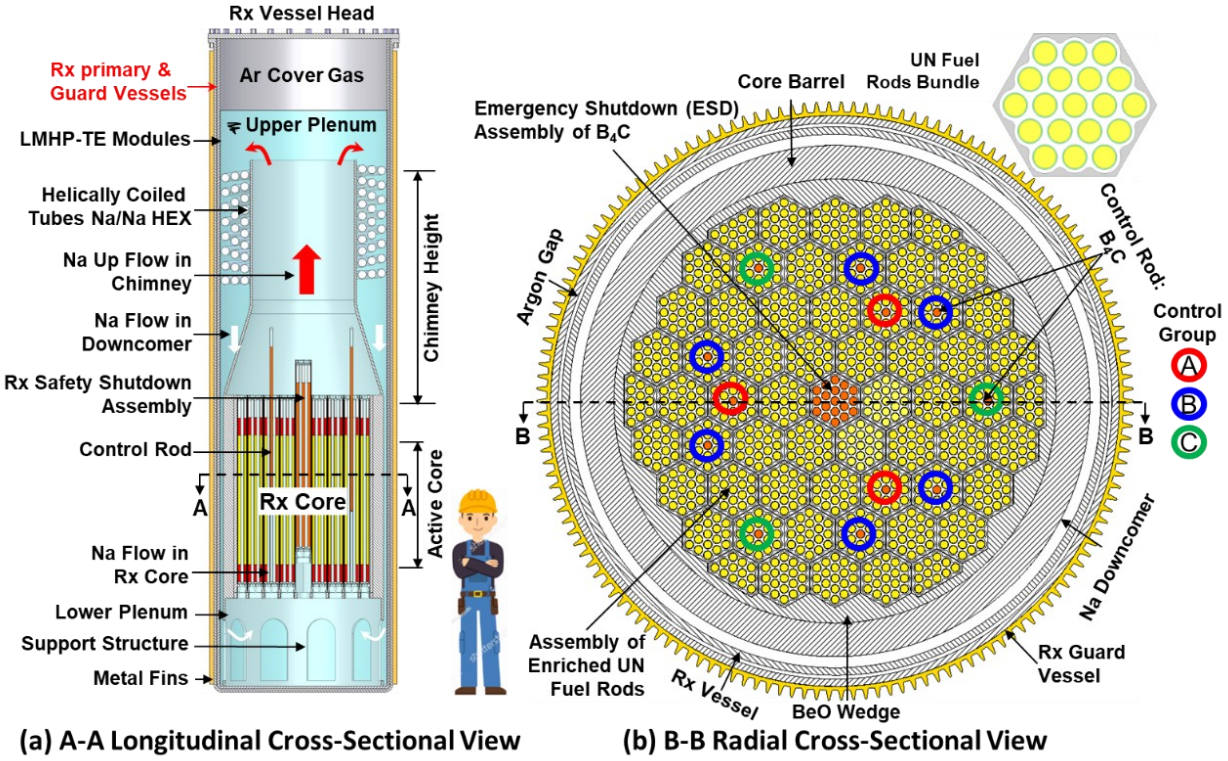

Fig. 2. Longitudinal and radial cross section views of the VSLLIM microreactor for generating 1-10 MW_{th}: (a) natural circulation of in-vessel liquid sodium and (b) primary control rod groups and the ESD assembly [modified from El-Genk, Schriener, and Palomino 2021].

Owing to the low vapor pressure of liquid sodium, the VSLLIM microreactor operates below atmospheric pressure, which eliminates the need for a pressure vessel. Instead, it has primary and guard vessels or containments separated by a small gap filled with argon gas to house sodium leak detectors and decrease side heat losses during reactor operation. In the event of a loss of heat removal, due to a failure or malfunction of the in-vessel Na/Na HEX, the argon gas in the gap between the primary and guard vessels is replaced with liquid sodium. This facilitates the decay heat removal by in-vessel natural circulation of liquid sodium and by natural circulation of ambient air along the outer surface of the guard vessel (Fig. 3) [Serrano De Caro 2012].

The VSLLIM microreactor core (Fig. 2b) loaded with hexagonal assemblies of 13.76 wt.% enriched UN fuel rods with HT-9 steel cladding and with scalloped BeO walls (Fig. 4). The walls help achieve a laterally uniform liquid sodium flow for cooling the fuel rods within the assemblies [El-Genk and

Palomino 2019]. The fifty-four full hexagonal assemblies and the six partial assemblies of UN fuel rods are arranged in the reactor core in four concentric rings (Fig. 2b). The full assemblies are loaded with 19 UN fuel rods each and the partial corner assemblies contain 12 UN fuel rods each. The BeO wedges surrounding the UN fuel assemblies within the HT-9 steel core barrel, serve as radial neutron reflectors (Fig. 2b).

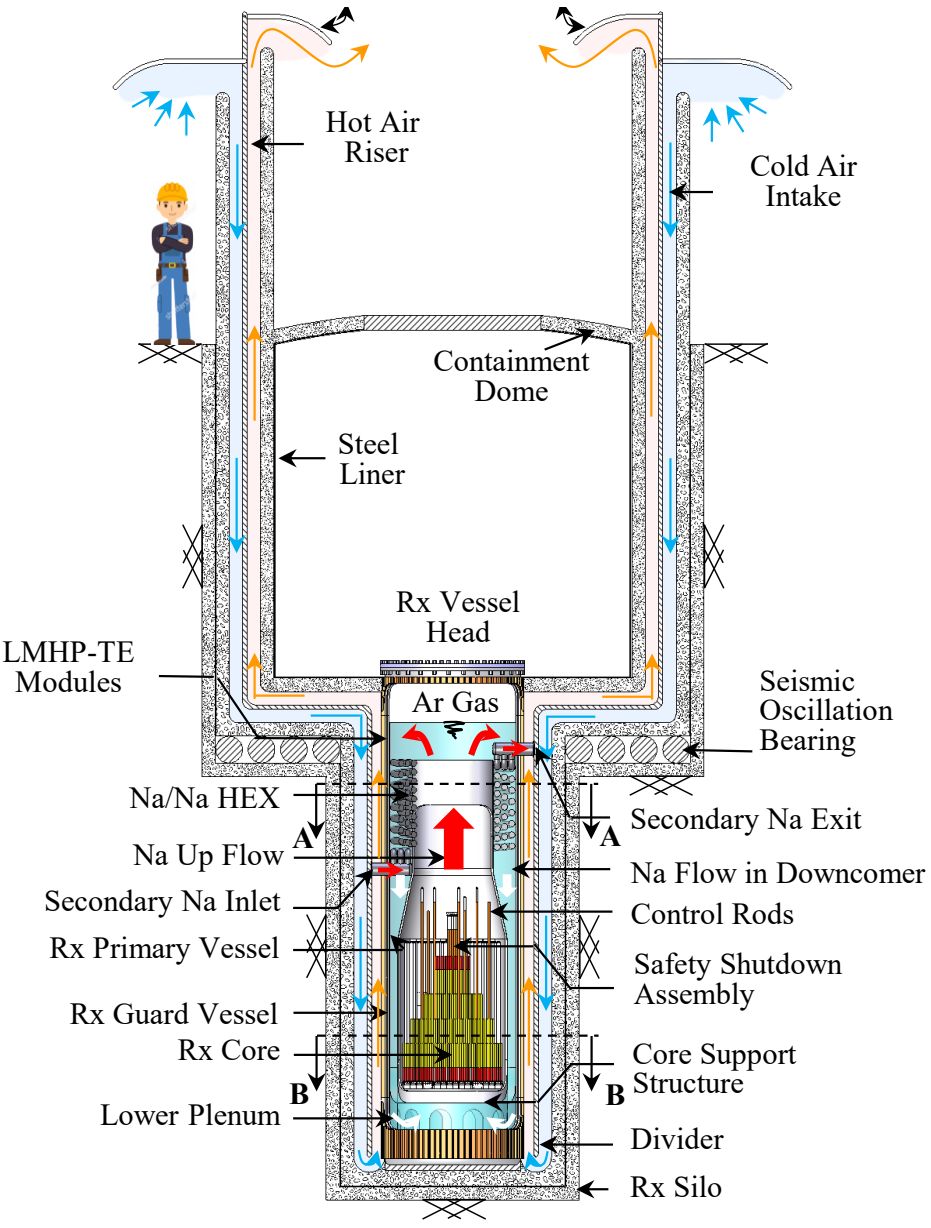

Fig. 3. Longitudinal cross-section of the VSLLIM microreactor installed below ground and mounted on seismic isolation bearings [El-Genk and Palomino 2019].

The VSLLIM microreactor has two independent and redundant means for the reactor control. The twelve B_4C Reactor Control (RC) rods located at the center of selected UN fuel assemblies in the second and third rings of the core (Fig. 2b, 4a and 4c) are for reactor control during operation and shutdown. These control rods fall into three groups, labeled A, B, and C, with separate drive motors (Fig. 2b). Group A

comprises three B_4C rods located at the center of fuel assemblies in the second ring of the reactor core. Group B comprises six B_4C rods in fuel assemblies in the third ring of the core, and Group C comprises three B_4C rods in the fuel assemblies in the third ring of the core (Fig. 2b).

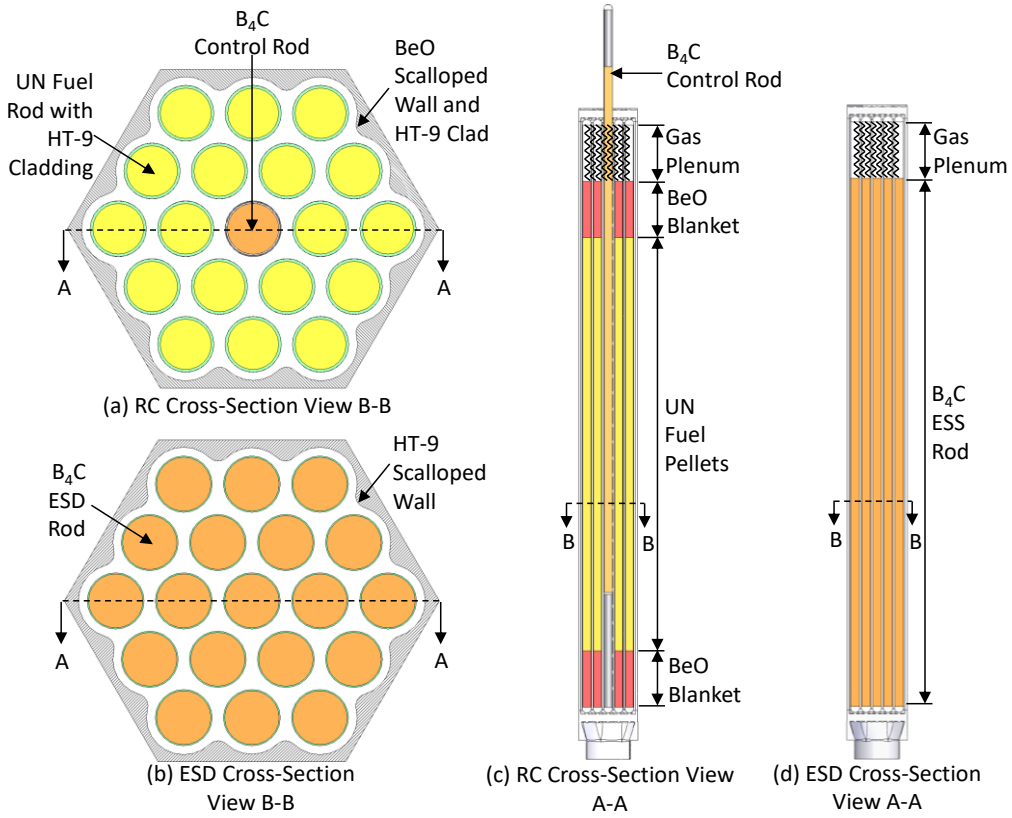

Fig. 4. Cross section and elevation views of a UN fuel assembly with central B_4C control rod (4a, 4c) and the central ESD assembly of 19 B4C rods (4b, 4d). [modified from El-Genk and Palomino 2019]

The central Emergency Shut Down (ESD) assembly of 19 B_4C rods, 80% enriched in ^{10}B, within scalloped HT-9 steel wall (Fig. 2, 4b and 4d) provides independent shutdown of the reactor in case of an emergency. The next section briefly describes the VSLLIM microreactor digital twin dynamic model developed using the MATLAB Simulink platform [The Mathworks 2024]. This model is used for training and testing the SAC-FNN algorithms implemented into the PLC controller of the microreactor during simulated startup and operation transients.

3. VSLLIM Digital Twin Model and Controller

The VSLLIM digital twin dynamic model couples a 6-group point kinetics sub-model [El-Genk and Tournier 2016] that accounts for the temperature reactivity feedback to thermal-hydraulics sub-models of the VSLLIM microreactor and the in-vessel Na/Na HEX (Figs. 2a and 5). The digital twin model uses the versatile MATLAB Simulink platform [The Mathworks 2024] to solve the governing equations in the coupled sub-models. The determined values of the physics-based operation parameters during the simulated startup transients are used for training the ML algorithms. These parameters are the reactor thermal power, the average temperatures of the UN fuel, HT-9 steel cladding and structure and the

circulating in-vessel liquid sodium in the reactor core, the mass flow rate and the temperature of the liquid sodium exiting the reactor core, and the temperatures of the rising sodium in the chimney, in the upper and lower plenums and on the shell side of the in-vessel Na/Na heat exchanger (Figs. 2-4). The Na/Na HEX maintains the temperature of the in-vessel liquid sodium entering the core at a 610 K while the exit temperature that varies with the reactor thermal power is < 800 K. At these temperatures liquid sodium is compatible with the HT-9 steel cladding of the UN fuel rods and core structure [Serrano De Caro 2012]. The VSLLIM digital twin model uses the ode23s modified Rosenbrock solver in the MATLAB-Simulink platform [The Mathworks 2024] to numerically solve the coupled point-kinetics sub-model to the overall energy and momentum balance equations of the reactor (Fig. 5) with 20 ms time step size during the simulated transients.

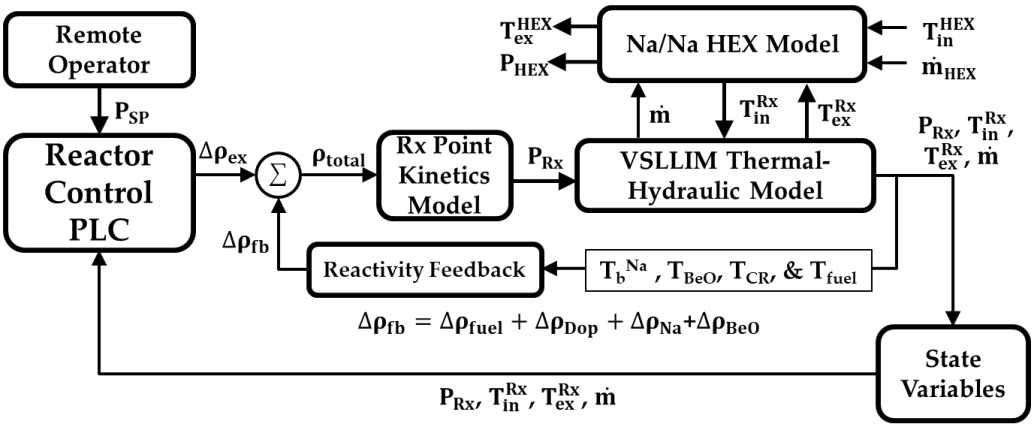

Fig. 5. A block diagram of the coupled sub-models in the MATLAB Simulink VSLLIM microreactor digital twin model [El-Genk, Schriener, and Shaheen 2025].

The 6-group point-kinetics sub-model calculates the transient changes in the reactor fission power, P_{Rx}, as a function of the external reactivity insertion, $\Delta\rho_{ex}$, and the temperature reactivity feedback, $\Delta\rho_{fb}$. The simulated startup transient of the VSLLIM microreactor begins after fully withdrawing the ESD central assembly. The inserted external reactivity is due to partially withdrawing the Groups A, B, and C control rods in the core. The temperature reactivity feedback, due to the decreases in the densities of the fuel, cladding, liquid sodium, in the reactor core and the Doppler broadening of the neutron cross sections in the UN fuel, are highly negative. However, the temperature reactivity feedback of the BeO in the radial and axial reflectors and in the scalloped walls of the UN fuel assemblies is slightly positive [El-Genk and Palomino 2019]. In the simulated startup transients, the total reactivity, ρ_{total}, in the VSLLIM microreactor core is the sum of the external reactivity inserted and the total temperature reactivity feedback (Fig. 5).

The thermal-hydraulic sub-model of the reactor simultaneously solves the coupled energy balance equations in the UN fuel rods, core structure, and the in-vessel sodium and the momentum balance equation for natural circulation of the in-vessel liquid sodium coolant in the reactor core, chimney and the downcomer. The sub-model of the Na/Na HEX (Fig. 5) simultaneously solves the energy and momentum balance equations of the secondary liquid Na flowing inside the helically coiled tubes of the Na/Na heat exchanger and the in-vessel liquid sodium flow on the shell side of the HEX [El-Genk and Palomino 2019].

The VSLLIM digital twin incorporates sub models for simulating the effects of fuel burnup into the reactor kinetics model, modeling decay heat generation for reactor shutdown transients, and varying the load demand in the submodel of the Na/Na HEX. The burnup reactivity submodel calculates the decrease in excess reactivity for the VSLLIM reactor as a function of the total energy generated in the fuel, or its burnup, in units of energy (MWd). The digital twin implements reactivity depletion rates determined by performed fuel depletion analysis of the VSLLIM microreactor [El-Genk, Palomino, and Schriener 2017] at different thermal power levels using the MCNP6 code version 1.0 [Goorley 2014].

3.1. The VSLLIM Reactor Controllers

During simulated startup transients, the Reactor Control PLC commands the VSLLIM digital twin (Fig. 5) and determines the rates and the magnitudes of the axial displacements of the ESD assembly and Groups A, B, and C control rods in the reactor core (Figs. 2 – 4). The PLC receives commands from the remote operator to start up or shut down the VSLLIM microreactor as well as the desired reactor power setpoint, P_{SP} (Fig. 5). The digital twin model calculates the magnitude and the rate of the external reactivity insertion, $\Delta\rho_{ex}$, in the reactor core as a function of the axial displacements of the control rods in the reactor core and fed it to the point-kinetics sub-model (Fig. 5). The controller continues to adjust the axial displacement of control rods until reaching the operator specified setpoint, P_{SP}, of the reactor thermal power.

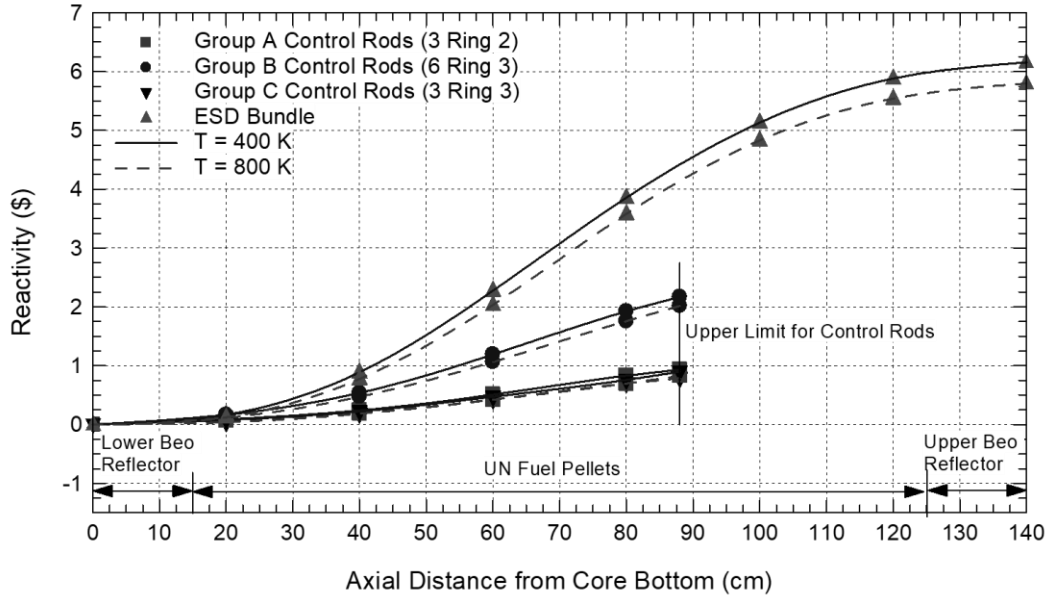

Fig. 6. Reactivity worth of the VSLLIM control rod groups and the ESD central assembly versus axial displacement in the reactor core at mean temperatures of 400 and 800 K [El-Genk, Schriener, and Shaheen 2025].

The results in Fig. 6 are those of the performed neutronics analyses using the MCNP6 code [Goorley 2014] to determine the reactivity worth of each of the control rod groups in the VSLLIM reactor core as a function of axial displacement from the bottom of the core and the calculated mean temperatures in the core (Fig. 6). This figure plots the calculated reactivity worth of the control rods in Groups A, B, and C and of the center ESD assembly as functions of axial displacement at isothermal temperatures of 400 K

and 800 K. The vertical line in the figure marks the limit set for the axial withdrawal of the B_4C control rods in the core, which corresponds to 2/3 the active core height to speed up reactor shutdown in case of an emergency. The results assume that the control rods are in thermal equilibrium with the in-vessel liquid sodium in the reactor core.

3.1.1. Reactor Control PLC

Two Reactor Control PLC programs are developed to determine the control element positions, using (a) a modified Proportional-Differential (PD) controller used for generating the target data for training and (b) a ML controller using the trained SAC-FNN algorithms. The Reactor Control PLC program runs with a scan cycle time of 50 ms, which is sufficiently small to capture the response of the PLC to changes in the reactor operation. At the start of each scan cycle, the PLC reads the Modbus input registers holding the calculated values of the VSLLIM reactor state variables by the digital twin and the commands received from the remote human operator. The state variables include the reactor thermal power, the in-vessel and HEX Na flow rates, the core Na inlet and exit temperatures, the HEX Na inlet and exit temperatures, the calculated core reactivity, and the axial positions of the control rod groups and the ESD assembly. The PLC then acts on the received commands from the remote operator to determine the displacement rates for the control elements. At the end of the scan cycle the actions to move the control elements are written to the PLC's Modbus output holding registers and communicated to the digital twin model of the VSLLIM microreactor.

During the simulated startup transients, the Reactor Control PLC brings the digital twin from an initial cold subcritical condition at a mean core temperature of 500 K to a steady full power operation at the reactor power setpoint specified by the remote operator. The PLC adjusts the axial displacement of the control rods to bring the reactor power to the setpoint specified by the remote operator, P_{SP}.

The Reactor Control PLC with the modified PD controller adjusts the rate of axial displacement of the control rods to within ± 0.125 mm/s, depending on the input value of $(P_{SP} - P_{Rx})$. The modified PD controller uses a criterion derived from that proposed by Bernard, Lanning, and Ray [1984] to adjust the axial withdrawal of the control rods to ensure smooth and gradual increase in the total reactivity, ρ_{total}, and hence in the reactor power and temperatures, during the startup transient. This criterion is given as:

$$\rho_{total} < \frac{1}{\alpha}\left[\frac{\left|\frac{d\rho}{dt}\right|}{\lambda_e} + \left|\frac{d\rho}{dt}\right| \tau \ln\frac{P_{SP}}{P_{Rx}}\right], \quad (1)$$

In this expression, α is a scaling coefficient, $\frac{d\rho}{dt}$ is the rate of change in the total reactivity, τ is the reactor period, and λ_e is the effective decay constant for the six delayed neutron groups in the reactor's point-kinetics sub-model. The scaling coefficient provides adequate time for the total reactivity to account for the delayed negative temperature reactivity feedback due to the thermal inertia of the system before further displacing the control rods. A value of $\alpha = 25$ is used in the present work, for a good balance between shortening the startup time and ensuring smooth increases in the reactor thermal power and the core temperatures during the simulated startup transients.

The Reactor Control PLC program incorporating the SAC-FNN algorithms inputs the current state variables to the trained neural network and determines the position of the reactor control elements from the network's output. The movement rate of the Group A and C control rods is determined from the

difference between the desired control rods' displacement and the present axial displacement. This displacement is restricted by the same ± 0.125 mm/s limit for the PD controller. Unlike the PLC with PD controller, the PLC program with the ML algorithms does not explicitly limit the control rod displacement using the restriction criteria in Eq. (1). Instead, the PLC relies on the trained SAC-FNN algorithm to adjust the control rod positions and ensure a smooth increase or decrease in the reactor power.

3.1.2. HEX Secondary Flow PLC

In addition to the Reactor Control PLC, the VSLLIM microreactor has a PLC that adjusts the secondary Na flow in the Na/Na HEX. It uses a Proportional-Integral (PI) control function to regulate the Na flow rate inside of the helically coiled tubes (Fig. 2). This function maintains the temperature of the in-vessel liquid Na entering the reactor core, T_{in}, constant at ~610 K. The input to the HEX PLC PI controller is the difference between the current in-vessel Na inlet temperature to the reactor core, T_{in}, and the setpoint of 610 K.

3.2. A Simulated Startup Transient of VSLLIM Microreactor

The VSLLIM microreactor digital twin model (Fig. 5) simulates reactor startup from an initial subcritical condition to steady state operation at a user specified reactor thermal power setpoint. Fig. 7 presents the results of a simulated startup transient based on the control rods' reactivity worths in Fig. 6. The startup transient in Fig. 7 begins with the reactor initially subcritical with the in-vessel liquid sodium and the reactor core at 500 K. The Reactor Control PLC first fully withdraws the ESD center assembly from the reactor core over a period of 240 s (Point 1 in Fig 7a). At such point, the reactor is still subcritical. Then the Reactor Control PLC axially withdraws the Group B control rods by 0.77 m over a period of 180 s for the reactor to achieve criticality (Point 2 in Fig. 7a). Next, the PLC simultaneously withdraws Group A and C control rods in the reactor core at a constant rate of 0.75 mm/s until the reactor power reaches a steady value of 100 kW_{th} (Point 3 in Figs. 7a and b). Subsequently, the PD controller manages the withdrawals of the control rods to bring up the reactor power to the setpoint $P_{SP,1}$ = 0.5 MW_{th}. The PLC limits the movement rate of the Group A and C control rods to 0.125 mm/s to ensure a smooth rise of both the reactor power and the exit temperature of the in-vessel liquid Na in core (Figs. 7b and c). The Na/Na HEX PLC increases the flow rate of the secondary liquid sodium in the helically coiled tubes to maintain the inlet temperature of the in-vessel sodium into the reactor core, T_{in}, at 610 K (Fig. 7c and d). The VSLLIM reactor reaches a steady state power of 0.5 MW_{th} at t = 2.38 hr. into the startup sequence (Fig. 7b).

The VSLLIM reactor operates at the power setpoint of 0.5 MW_{th} for a period allowing the remote operator and the on-site diagnostics to check out the systems prior to resuming the increase in the reactor power to 10 MW_{th}. The remote operator sends a command to the reactor controller to increase the reactor thermal power setpoint from 0.5 MW_{th} to 10 MW_{th} (Point 6 in Fig. 7). The PD controller simultaneously displaces the Group A and C control rods to increase the external reactivity insertion and hence the reactor thermal power (Figs. 7a and b), the circulation rate of the in-vessel liquid sodium, and the sodium exit temperature from the reactor core. The values of these parameters increase steadily over a period of 4.75 hrs. until the reactor power reaches and levels off at 10 MW_{th} (Point 7 in Fig. 7). The corresponding temperature and circulation rate of the in-vessel liquid sodium at the reactor core exit are 780.6 K, and

46.0 kg/s, respectively. The next section describes the training process and results for the SAC-FNN algorithms for the reactor control of the VSLLIM digital twin model.

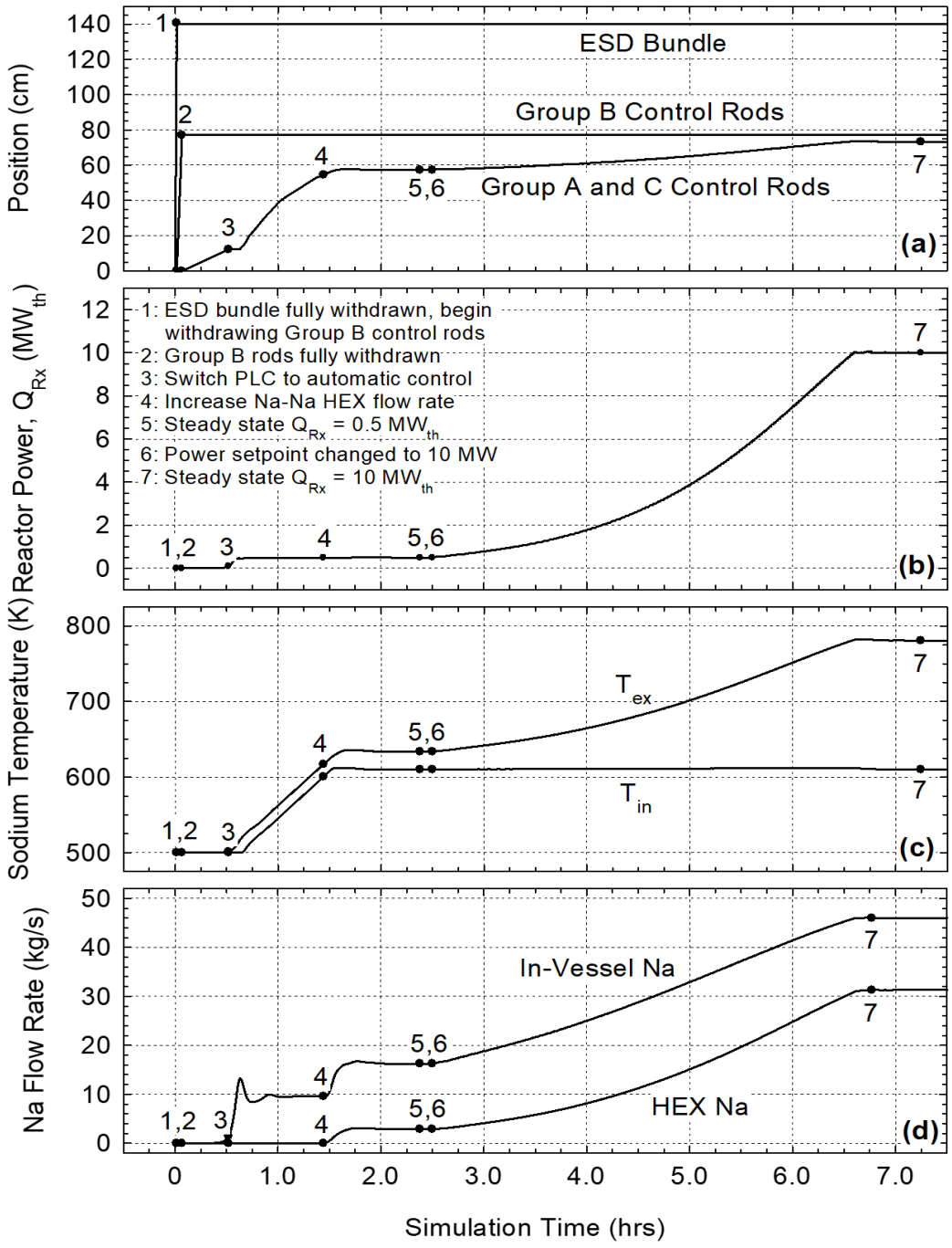

Fig. 7. Operation parameters of the VSLLIM microreactor during a simulated startup transient to a steady thermal power of 10 MW: (a) positions of the ESD assembly and the Group A, B, and C control rods, (b) the reactor thermal power, (c) the sodium temperatures at the inlet and exit of the reactor core, and (d) the mass flow rates of the in-vessel Na and the secondary Na in the helical coiled tubes of the Na/Na HEX [El-Genk, Schriener, and Shaheen 2025].

4. Training the SAC-FNN Algorithm

The FNN in the algorithm processes information in one direction, where the output values for a layer of neurons pass on to the inputs of the next layer of neurons (Fig. 8). The network output of FNNs is solely based on the present values of the features, F (Figs. 8a and 8b). The features used for training the SAC-FNN in this work are the reactor thermal power, Q_{Rx}, the reactor core exit temperature, T_{ex}, and the in-vessel sodium flow rate, $\dot{m}$. The Actor Network comprises an input layer with a single neuron, three hidden layers of many neurons each, and an output layer with two neurons (Fig. 8a). For each feature value, x, the normalized value, X*, is calculated using a min-max normalization function:

$$x^* = \frac{x - x_{min}}{x_{max} - x_{min}} \quad (2)$$

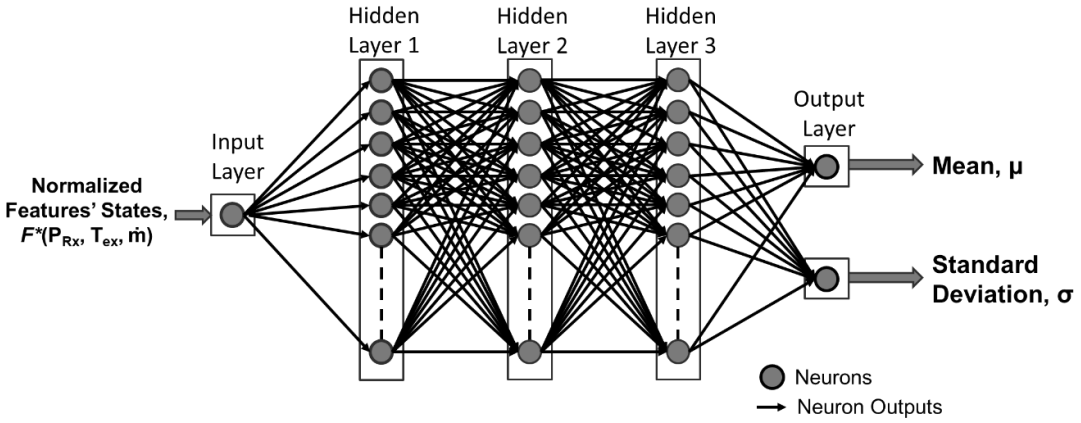

(a) Feedforward Neural Network Structure for the SAC Actor Network

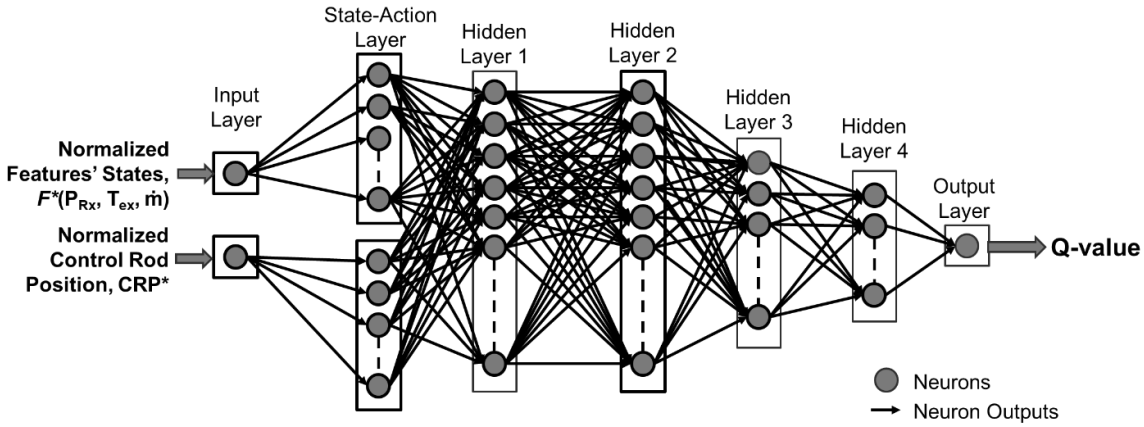

(b) Feedforward Neural Network Structure for the SAC Critic Network

Fig. 8. Feedforward Neural Network structures of the (a) Actor and (b) Critic networks used in SAC-FNN algorithm [El-Genk, Schriener, and Shaheen 2025].

The array of normalized features, F*, passes through the input layer (Fig. 8a) which passes the output values to the neurons in the first hidden layer. The output values, Y, are calculated from input values, X, based on the values of the neurons' weight, w, and bias, b, and an activation function α, as:

$$Y = \alpha(w\,X + b) \tag{3}$$

The SAC-FNN algorithm updates the learned weight and bias parameters of the neurons in the FNNs during the training process. The mean (μ) and standard deviation (σ) output by the Actor Network define a normal distribution of the normalized control rod displacements (Fig. 8a). The two neurons in the input layer of the Critic Network are for the array of the normalized state values, F*, and the corresponding normalized control rods position CRP* (Fig. 8b). These values pass through the neurons in the State-Action layer and sequentially to each of the four hidden layers for the Critic Network. The output layer calculates the approximate action function, referred to as the Q-value.

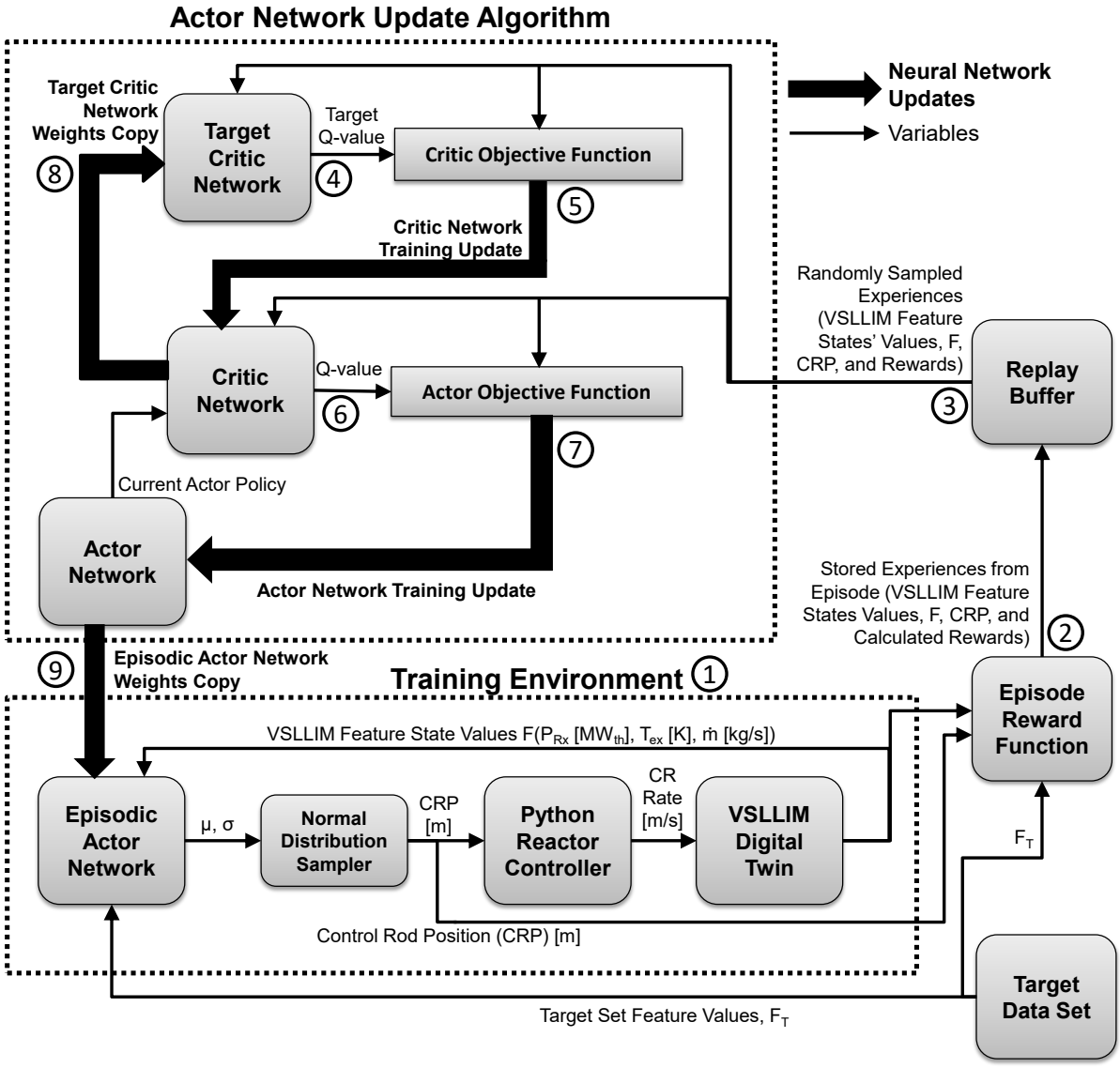

Fig. 9. A block diagram of the training process of the implemented SAC-FNN algorithm [El-Genk, Schriener, and Shaheen 2025].

The SAC-FNN algorithm is incorporated into a Python program using Tensorflow [Abadi 2016] with the Keras ML libraries [Chollet 2015] based on those proposed by Bae, Kim, and Lee [2023]. These include a

Training Environment and an Actor Network Update Algorithm (Fig. 9). The Training Environment (Point 1 in Fig. 9) couples the Episodic Actor Network to the Python Reactor Controller (described in Section 3.1). The environment links the controller to the VSLLIM digital twin model to control the movement of the control rods during the performed transient startup scenario (Fig. 7). During each training episode the controller attempts to follow the startup scenario in the user supplied Target Data Set and bring the VSLLIM microreactor to the specified target power setpoint, P_{sp}. The trained SAC-FNN algorithm learns to reproduce the startup control actions of the PD controller displayed in the Target Data sets (Fig. 9). These sets are generated by the digital twin model of the VSLLIM microreactor (Fig. 5).

In each timestep of the simulated startup transient (e.g., Fig. 7), the Episodic Actor Network (Fig. 8a) receives the features, F, from the VSLLIM digital twin model (Fig. 5) and the mean and standard deviation of the output data. The Normal Distribution Sampler then samples a CRP* from the developed normal distribution of the calculated values of μ and σ. These values are de-normalized using the defined min-max de-normalization (Eq. 2) and pass on to the Python Controller. The controller calculates the displacement rates of the Group A and C control rods in the core of the VSLLIM microreactor (Fig. 2) based on the difference between the predicted and the actual positions of the control rods. The controller limits the displacement rate of the control rods to 0.125 mm/s and communicates the displacement rate of the control rods to the digital twin model to adjust the reactor operation parameters in the next simulation timestep. The Python Controller communicates with the digital twin using a POSIX shared memory function. The MATLAB engine for python [The Mathworks 2022] launches the digital twin model of the VSLLIM reactor at the start of each training episode (Fig. 9).

The algorithm randomly selects sets of the features at different points of the episode, the corresponding predicted control rods position, and the calculated rewards at the end of each episode. It stores these values, referred to as experiences, within the Replay Buffer. The experiences stored are of the current and all previous training episodes. The SAC-FNN algorithm randomly samples a batch of experiences from the Replay Buffer and passes them to the Actor Network Update function to update the Actor Network to improve its performance. The update function comprises the Actor Network, the Critic Network, and the Target Critic Network (Fig. 9).

The Actor Network learns a policy to determine the control actions, the Critic Network learns the action-value function (called the Q-value function) to update the policy of the Actor Network, and the Target Critic Network helps stabilize the Critic Network by evaluating its performance in updating the policy of the Actor Network. The Target Critic Network calculates a target Q-value (Point 4 in Fig. 9) that passes on to the Critic Objective Function to estimate the expected future reward for the Actor Network. This value is compared to past reward values to determine the updates for the weight and bias matrices in Critic Network (Point 5 in Fig. 9).

The updated Critic Network uses sampled experiences from the Replay Buffer and the policy actions of the Actor Network to calculate the Q-value for the Actor Objective Function (Point 6 in Fig. 9). It then updates the weights and biases in the Actor Network to maximize the episodic reward (Point 7 in Fig. 9). The SAC-FNN algorithm copies the parameters of the Critic Network to the Target Critic Network to improve the controller's behavior in the next episode (Points 8, 9 in Fig. 9). The process continues in subsequent episodes until the SAC-FNN algorithm successfully trains the Episodic Actor Network. A successful episode is the one in which the Episodic Actor Network of the trained SAC-FNN algorithm

successfully increases the thermal power of the VSLLIM microreactor during the simulated startup transient from an initial setpoint $P_{sp,1}$ = 0.5 MW_{th}, to the final setpoint $P_{sp,2}$ =10.0 MW_{th}.

4.1. Implemented SAC-FNN Algorithm Results

The implemented SAC-FNN algorithm performed 25 different training runs or cases, labeled A-Y. The five cases labeled A-E are for troubleshooting and optimization prior to conducting the actual training cases labeled F through Y. Table 1 lists selected and varied hyperparameters in the SAC-FNN training cases. The performed parametric analyses for the SAC-FNN algorithms investigate the effects of the number of neurons in the hidden layers of the Actor Network and the Critic Networks. The Actor Networks each have three hidden layers of neurons (Fig. 8a), with a varied number of neurons per layer from 16 to 256 (Table 1). The number of neurons in the hidden layers of the Critic Networks varied commensurate with those of the Actor Network to 256, 512, 256, 128, 64 for the state action layer and four hidden layers (Fig. 8b). The performed analyses also investigate the effect of employing initial weights for the Actor and Critic Networks that are either randomly determined using the Xavier uniform distribution or taken from the values for a previously successful episode. The trained SAC-FNN algorithms successfully complete the transient startup of the VSLLIM microreactor using both randomly determined wights and selected weights from previously successful episodes.

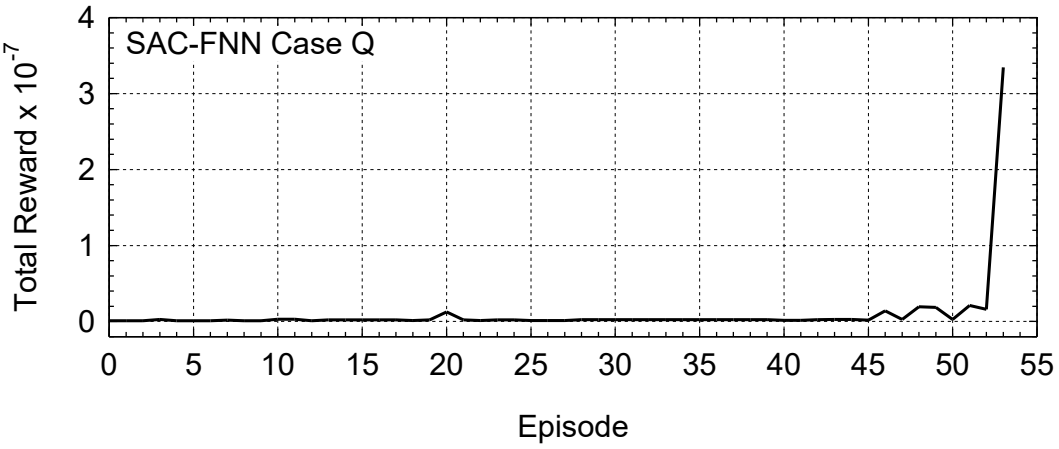

Fig. 10. Example of progression of total episodic reward for the SAC-FNN Training Case Q [El-Genk, Schriener, and Shaheen 2025].

As an example of the training results, Fig. 10 plots the changes in the episodic reward during the training case Q. The small initial reward is due to the early termination of the episodes when one of the state variables, either the reactor thermal power, the reactor Na exit temperature, or the in-vessel Na mass flow rate, continuously exceeds the specified termination range for period of 60s. Eventually, the trained SAC-FNN algorithms successfully completes the simulated startup transient in episode 54, as indicated by the large total reward.

Not all performed training cases produced successful episodes in which the SAC-FNN algorithms complete the VSLLIM startup scenario to the final reactor power setpoint of 10.0 MW_{th}. Thirteen successfully trained algorithms are produced during 25 training cases of the SAC-FNN algorithm. The results of the performed parametric analyses of varying the number of neurons per layer showed that only

the networks with 3 layers and 64 and 256 neurons per layer produced successful training cases. The training cases R, X, and Y with networks of 64 neurons per layer produced a total of nine successful episodes. The training cases K, P, and Q with networks of 3 layers and 256 neurons per layer produced four successful episodes. The training cases with networks of 3 layers of only 32 and 16 neurons per layer did not produce any successful episodes.

Figure 11 plots the predicted position of the Group A and C control rods in the core of the VSLLIM microreactor by the trained SAC-FNN algorithm versus the target values in the simulated startup transients. The nine successfully trained SAC-FNN algorithms, each of 3 layers and 64 neurons per layer in cases R, X, and Y accurately predict the control rods' position to within +0.3% and -1.6% of the target (Fig. 11a-c). The four successfully trained SAC-FNN algorithms of 3 layers and 256 neurons per layer in cases K, P, and Q accurately predict the position of the control rods within +0.5 % and -1.2% of the target values (Fig. 11d).

Table 1. Listing of the selected hyperparameters for training the SAC-FNN algorithms.

Hyperparameter	Value
Constant Hyperparameters	
Number of VSLLIM environments	1
Tolerance time	60 s
VSLLIM state space	3
VSLLIM action space	1
Maximum number of episodes per case	5,000
Maximum number of epochs per policy update	10,000
Hidden layers activation function	ReLU
Standard deviation layer activation function	Softplus
L2 weight regularization factor	0.01
Replay buffer storing frequency	1 s
Batch size	256
Optimizer	Adam
Learning rate	0.00001
Tradeoff coefficient learning rate	0.000005
Tradeoff coefficient initial value	0.5
Discount rate	0.99
Target smoothing coefficient, τ	0.001
Varied Hyperparameters	
Initialization of Actor and Critic Weights	Random using the Xavier uniform distribution, Weights successful actors and critics.
Number of Neurons in the Actor's Three Hidden Layers	(256, 256, 256), (64, 64, 64), (32, 32, 32), (16, 16, 16)
Numbers of Neurons in the Critic's state-action layers and Four Hidden Layers	(256, 512, 256, 128, 64), (64, 64, 32, 16, 8), (32, 32, 16, 8, 4), (16, 16, 8, 4, 2)

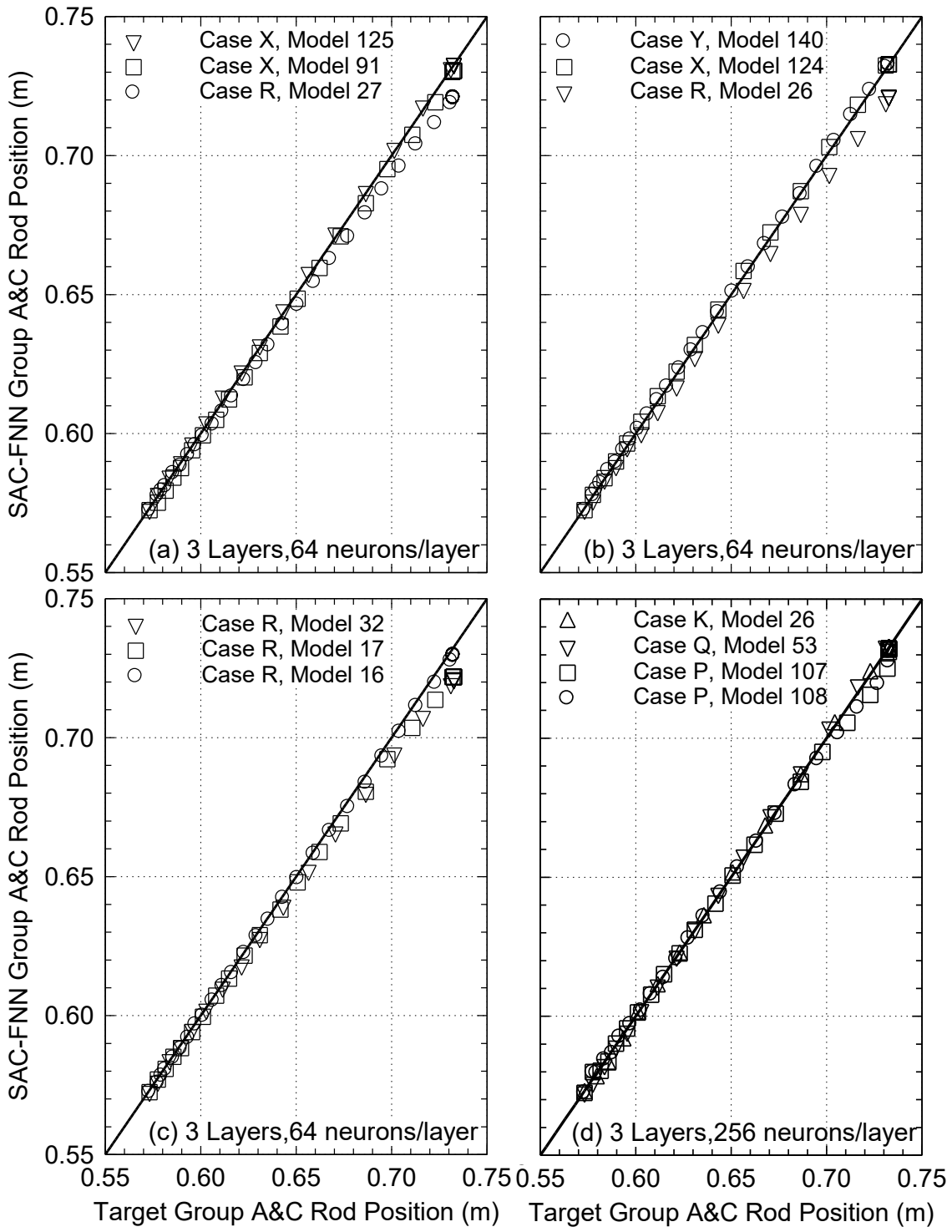

Fig. 11. Comparison of predicted positions of the Group A and C control rods of the VSLLIM microreactor by the trained SAC-FNN algorithms with (a-c) three layers, and 64 neurons per layer and (d) three layers, and 256 neurons per layer versus the target values in the simulated startup transients [El-Genk, Schriener, and Shaheen 2025].

5. Evaluating the Performance of the Trained SAC-FNN Algorithm in the Real Time Controller

The trained SAC-FNN algorithms are next integrated into the developed python program for the Reactor Control PLC to adjust the displacements of the control rods during the simulated startup transients using the VSLLIM digital twin model (Fig. 5). During testing, the digital twin model runs synchronously to a real-time clock with a small timestep of 20 ms to produce a fine temporal discretization and a better approximation of a continuous data source. This allows the PLC to interact effectively and realistically with the VSLLIM digital twin model. The actions of the PLC are delayed by the time required for the signals of the reactor operating parameters to reach the controller, and for the generated control signals reach the digital twin model of the reactor, providing a more realistic testing environment for the controller. In the present work the values of the state variables generated by the digital twin model of the reactor and passed on to the PLC did not include artificial sensor noise.

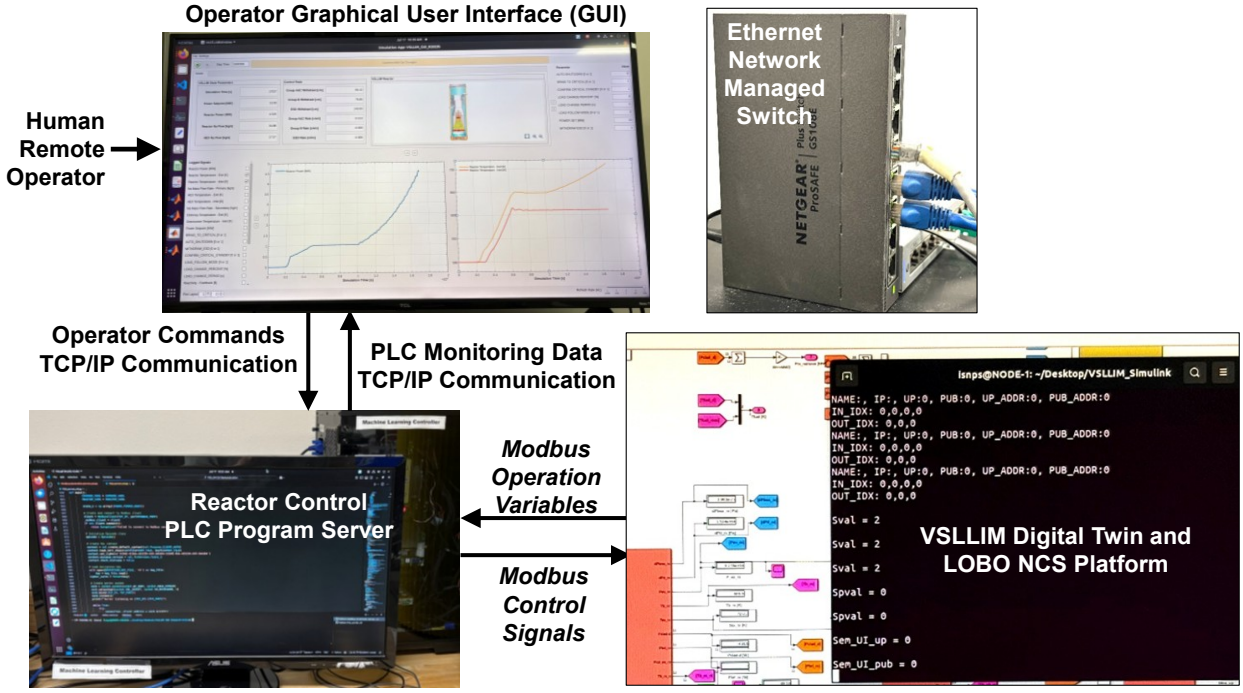

Fig. 12. Developed Setup for testing of the Reactor Control PLC with trained SAC-FNN algorithms and the MATLAB Simulink VSLLIM digital twin.

The LOBO Nuclear CyberSecurity (NCS) platform developed by University of New Mexico's Institute for Space and Nuclear Power Studies (UNM-ISNPS) in collaboration with Sandia National Laboratory [El-Genk and Schriener 2022; Schriener and El-Genk 2022; El-Genk, Altamimi, and Schriener 2021] links the Reactor Control PLC to the digital twin model of the VSLLIM reactor (Fig. 5). This platform uses the Modbus Industrial Control System (ICS) protocol to manage communication through an isolated Ethernet test network. This is between the PLC program and the server running in real-time, the digital twin model of the VSLLIM microreactor (Fig. 12).

The Modbus communication channel for the LOBO NCS data broker receives the calculated values of the state variables from the reactor digital twin model and stores them in Modbus holding registers (Fig. 12). It also passes the Modbus control signals sent by the PLC to the digital twin model, which then enacts the

transmitted control signal and displaces the control rods in the reactor core. The measured latency time of the Modbus communication between the PLC and the VSLLIM digital twin model in the ethernet testing network is ~ 0.2 ms on average.

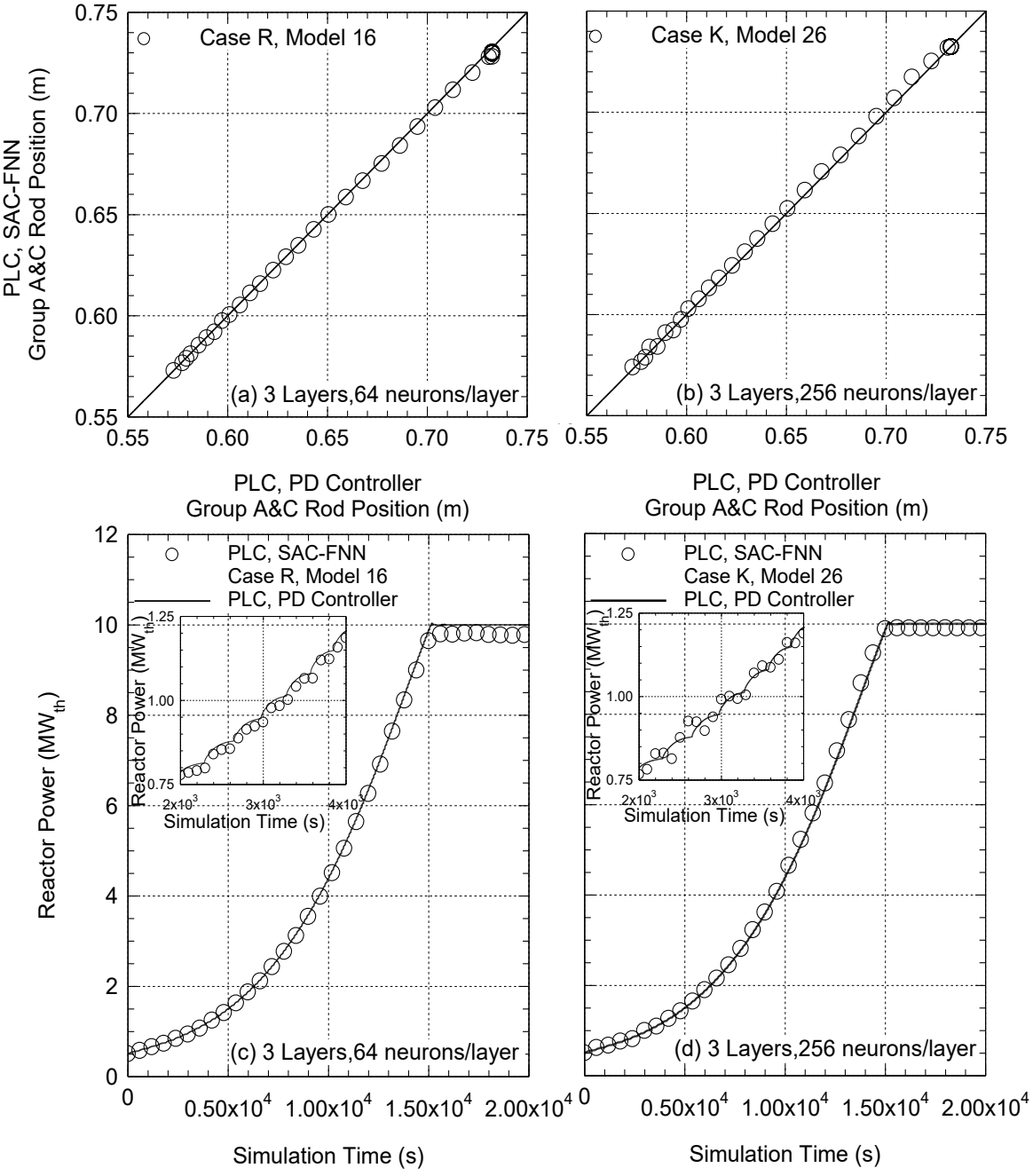

Fig. 13. Comparison of predicted positions of Group A and C control rods and the reactor power by the trained SAC-FNN algorithms incorporated into the Reactor Control PLC to those using the PLC with PD controller during a simulated startup transient of the VSLLIM microreactor for (a, c) Case R with 3 layers, 64 neurons per layer, and (b, d) Case K with 3 layers, 256 neurons per layer [El-Genk, Schriener, and Shaheen 2025].

In each scan cycle the PLC reads the most recently received state variables in the holding registers, before passing them to the control logic program with the trained ML algorithms. They manage the movement of the Group A and C control rods in the core of the VSLLIM microreactor during the simulated startup transients using the digital twin model (Fig. 7). The PLC determines and implements the movement rate of the Group A and C control rods in the core of the VSLLIM microreactor. These are commensurate with the position the rode determined by the trained SAC-FNN algorithms. The program writes the commanded movement rates to the Modbus holding registers of the PLC and passes them back to the LOBO NCS data broker. The data broker in turn passes the commanded movement rates to the digital twin model through a shared memory communication bridge for action.

Presented results are the predicted position of the control rods in the VSLLIM microreactor core by the successfully trained SAC-FNN algorithm and of the corresponding reactor thermal power determined by the digital twin model [El-Genk, Schriener, and Shaheen 2025]. These results are compared to those generated in the simulated startup transient of the VSLLIM microreactor connected to the PLC using the PD controller (Section 3.1.1). Figures 13a and 13b compare the predicted positions of the control rods in the case R model 16 and case K model 26 of the trained SAC-FNN algorithms of 3 layers of 64 and 256 neurons per layer, respectively, to those determined by the PLC with the PD controller. The PLC with the case R model 16 trained SAC-FNN algorithm slightly underpredicts the control rod positions to within -0.6% of the values determined by the PLC with the PD controller (Fig. 13a). At the end of the simulated startup transient, the reactor's thermal power determined using the PLC with SAC-FNN algorithm is 9.8 MW_{th} compared to the target of 10.0 MW_{th} (Figs. 13c).

The predicted positions of the control rods in the reactor core by the PLC with the case K model 26 trained SAC-FNN algorithm of 256 neurons per layer are in good agreement, to within +0.7% and -0.5% with the values calculated using the PLC with PD controller (Fig. 13b). The predictions of the PLC with the SAC-FNN algorithm levels off at a steady state reactor thermal power of 9.93 MW_{th}, slightly lower than the target of 10.0 MW_{th} (Fig. 13d). The inserts in Figs. 13c and 13d compare the small adjustments in the reactor power during the simulated startup transient. The rate limiting function of the PLC with the PD controller (Eq. 1) restricts the displacement of the Group A and C control rods to limit the change in the core external reactivity. Therefore, during the simulated startup transient the thermal power of the VSLLIM microreactor increases in small steps after accounting for the negative temperature reactivity feedback.

Although the PLC with the trained SAC-FNN algorithm does not have a rate limiting function (Eq. 1), it successfully learned to adjust the displacement of the control rods to increase the reactor power gradually without spikes (Figs. 13c and d). The PLC with the trained SAC-FNN algorithm of 265 neurons per hidden layer experiences larger oscillations in the predicted reactor thermal power in the startup simulation transient to 3,000 s. These oscillations are smaller for the startup transient controlled by the PLC with the trained SAC-FNN algorithm of 64 neurons per hidden layer (Figs. 13c and d). This is because the trained ML algorithms display slightly different behavior displacing the control rods during the simulated startup transient. Nonetheless, both algorithms predict similar rates of increase of the reactor power as the reference PLC with PD controller.

During the simulated startup transient of the VSLLIM microreactor, the results in Fig. 13 show that the trained SAC-FNN algorithms successfully control the movement of the Group A and C control rods (Fig.

2b) to increase the reactor power from 0.5 MW_{th} to a final setpoint of 10 MW_{th}. The other eleven successfully trained SAC-FNN algorithms incorporated into the PLC demonstrated similar behaviors, as those shown in Fig. 13. They smoothly increase the thermal power of the VSLLIM microreactor during the simulated startup transient to the final steady state power setpoint.

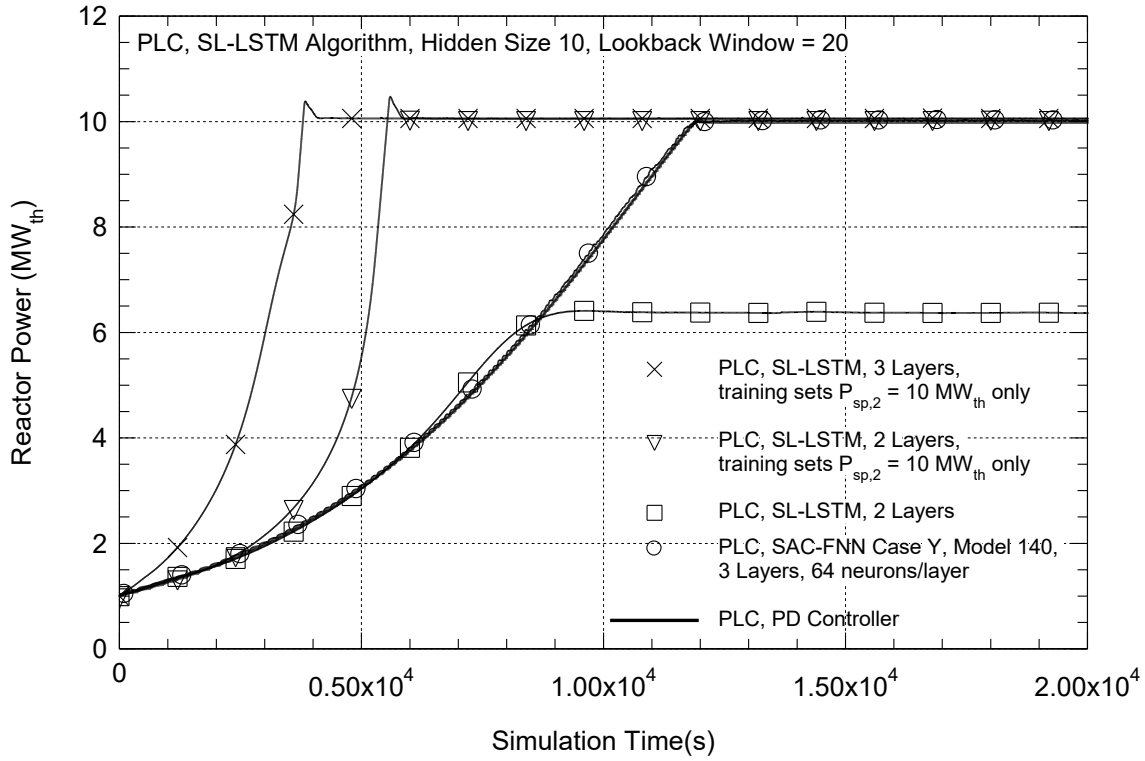

Fig. 14. Comparison of the predicted reactor thermal power during simulated startup transients using the Reactor Control PLC with the trained SL-LSTM and SAC-FNN algorithms to those calculated by the PLC with PD controller for the same power setpoint of $P_{SP,2}$ = 10 MW_{th} [El-Genk, Schriener, and Shaheen 2025].

5.1. Comparison of Results of PLC with the Trained SL-LSTM Algorithms

The VSLLIM Reactor Control PLC with the trained SAC-FNN algorithms performs well for real time control of the VSLLIM microreactor, showing significant improvement over the PLC with Supervised Learning and Long, Short-Term Memory (SL-LSTM) algorithms investigated in Task 1 [see details in El-Genk, Schriener, and Shaheen 2024, 2025]. Fig. 14 compares the predicted thermal power in a simulated startup transient using the PLC with both the trained SL-LSTM and SAC-FNN algorithms. The results presented for the trained SL-LSTM algorithms are for three different cases with a hidden size of 10 and a lookback window of 20 [El-Genk, Schriener, and Shaheen 2024]. In the simulated startup transient, the PLC increases the reactor power from an initial value of 1.0 MW_{th} up to 10 MW_{th}.

During the first 6,000 s of the simulated startup transient, the PLC with a trained SL-LSTM algorithm of 2 layers and the external reactivity, ρ_{ex}, as a feature [El-Genk, Schriener, and Shaheen 2025], increases the reactor power in good agreement with the predictions using the PD controller. However, the reactor power calculated by the digital twin model levels off at a steady state value of 6.37 MW_{th}, which is well

below the target setpoint of 10 MW_{th}. The PLC and the trained SL-LSTM algorithms with 2 or 3 layers, and ρ_{ex}, as a feature, reach the correct reactor power setpoint of 10 MW_{th}. However, they rapidly displace the Group A and C control rods causing the reactor power to rise faster than the target values calculated using the PLC with PD controller.

In contrast, the PLC with the trained case Y model 140 SAC-FNN algorithm of three layers and sixty-four neurons per layer smoothly increases the reactor power in close agreement with the predictions using the PLC with PD controller (Fig. 14). The reactor power levels off at a steady state value of 10.02 MW_{th}, only 0.2% higher than the target power setpoint. This acceptable performance for the trained Case Y SAC-FNN algorithm in Fig. 14 is consistent with those displayed for the cases K and R algorithms in Figs. 13 for real time control during the simulated startup transients.

The results for the Reactor Control PLC with the trained SL-LSTM algorithms show that despite the high testing accuracy of the algorithms [El-Genk, Schriener, and Shaheen 2024, 2025], the real-time control performance is poor and inconsistent (Fig. 14). The PLC with the trained SL-LSTM algorithms does not self-correct when the values of the input features differ from those in its training data sets. Owing to the highly nonlinear kinetics of the reactor, a slight change in external reactivity due to displacement of the control rods in the core results in larger changes in the reactor's thermal power and, hence, the features used to train the SL-LSTM algorithm. Examples are the reactor core exit temperature and the in-vessel Na flow rate through the core by natural circulation. Despite the high testing accuracy of the SL-LSTM algorithms during training and testing, a small difference in the predicted displacement of the control rods causes the reactor power to significantly deviate from the target values. The SL-LSTM algorithms do not incorporate control feedback during the training process but are trained using pre-generated data sets covering a wide range of target curves of the simulated startup transients with different reactor power setpoints. Consequently, the algorithms did not learn during training how the VSLLIM digital twin model responds to different predictions of the control rods positions from those in the training data sets. This contrasts with the trained SAC-FNN algorithms that learn to moderate the predicted displacements of the control rods and self-correct so that the increases in the reactor power agree with the target values (Figs. 13-14).

6. VSLLIM Digital Twin Secure Remote-Control Testbed

Safe, remote operation of the VSLLIM microreactor requires securing the TCP/IP communication signals between the remote operator workstation and the Reactor Control PLC in the reactor's digital control system. The values of the monitored reactor operation variables and command signals are combined into arrays of floating-point numbers and transmitted through the network as a series of TCP/IP packets. The secure communications scheme must prevent outside actors from conducting cyberattacks, sending false commands or monitoring signals to the operator or controller. It also needs to prevent outside observers from monitoring the data in the transmitted TCP/IP packets if they are intercepted while being transmitted. This information could be studied to learn how to generate realistic fake signals to try to disguise the plant's true conditions during a cyberattack attempt. Thus, the secure communication system needs to both ensure that the received signals came from the legitimate sources, as well as obscure the numerical values of these signals in the event the network traffic is intercepted.

The Reactor Control PLC with trained SAC-FNN algorithms demonstrated in the previous section is integrated into a testbed for demonstrating secure remote control of the VSLLIM digital twin model. The

developed testbed allows a human operator to monitor the operation of the simulated VSLLIM microreactor and send commands to the Reactor Control PLC to take actions. Figure 15 shows the elements of the developed remote-control testbed. The Reactor Control PLC with trained SAC-FNN algorithms runs on a Linux server connected to a separate Linux server running the MATLAB Simulink VSLLIM digital twin model (Figs. 12, 15). The Reactor Control PLC uses two communication channels: (a) a Modbus TCP channel which communicates with the LOBO NCS platform and (b) a TCP/IP channel for communicating with the remote operator workstation. The PLC's communication program serves as a TCP/IP host and accepts communication connection requests from the TCP/IP client program of the remote operator terminal (Fig. 15).

Once connected to the PLC, the remote operation terminal records operation variables received from the Reactor's Control PLC. The remote operator workstation comprises a Linux computer running a data communication program and the operator GUI, displayed on a large format monitor (Figs. 12, 15). The values pass to the GUI program using a POSIX IPC shared memory connection and are recorded locally in a data log. The operator sends commands back to the Reactor's Control PLC for implementation into the VSLLIM Digital Twin model. These commands include initiating start up, shut down, and changing the reactor power level.

During testing, the MATLAB Simulink transient model runs synchronously to a real-time clock with a timestep of 20 ms while the PLC program is configured to run with a scan cycle time of 50 ms. The VSLLIM reactor digital twin responds passively to load following operation, without actively moving the control rods, due to the inherent negative temperature reactivity feedback in the core. The operator can set the PLC to actively adjust the position of the control rods to reach a target reactor power setpoint. It can also be set to hold the position of the control rods constant when the reactor power changes passively during a load following transient.

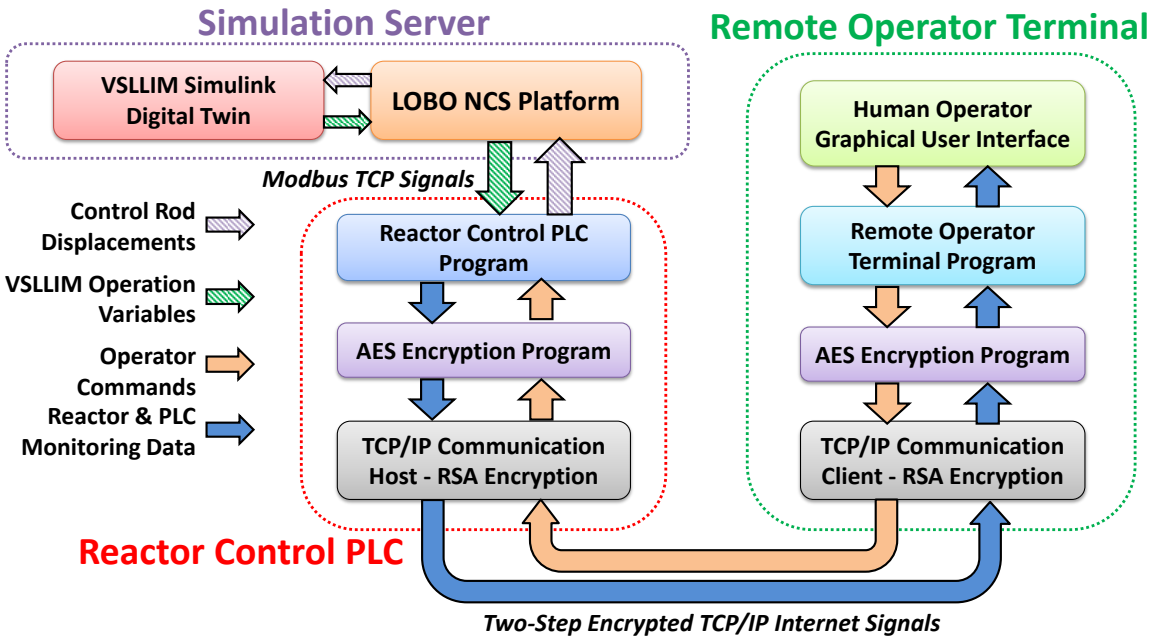

Fig. 15. Block diagram of secure remote-control concept for the VSLLIM digital twin.

The developed secure remote-control scheme for the VSLLIM microreactor implements a two-step data encryption scheme to secure the signals transmitted and received between the remote operator workstation and the communication program of the Reactor Control PLC (Fig. 15). The two-step system employs independent encryption methods, namely:

1. A symmetric encryption algorithm using AES (Advanced Encryption Standard) encryption keys for encrypting the data values prior to transmission and decrypting them after being received, and

2. An asymmetric encryption algorithm using RSA (Rivest–Shamir–Adleman) encryption keys for securing the TCP/IP data communication between the PLC (host) and operator workstation (client) processes.

6.1 AES Encryption Algorithm

The first layer of the secure communication setup employs AES encryption developed by the U.S. National Institute of Standards and Technology (NIST) [NIST 2001]. It uses symmetric encryption keys, where the same key is used for both encrypting and decrypting the data. The AES keys are generated using the 128-bit standard. The implemented algorithm encrypts the data in blocks of 128 bits for 10 rounds using the 128 bit-sized key. The encryption complexity resists any realistic brute force decryption attempt [Hathaway 2003]. The encryption keys are distributed to the computers running the Reactor Control PLC program and the remote operator workstation. They are transported on physical storage to avoid compromising the transmission and interception of the keys over a network connection.

The communication subroutines of the Reactor Control PLC and operator workstation collect the arrays of operator commands or reactor operation variables to be transmitted and pack them into structure objects, which are then encrypted using the AES key. Following transmission, the encrypted structure object containing the data is decrypted using the local copy of the AES key. If the received data has not been encrypted or is encrypted using a different AES key, the decryption program returns an exception error and logs the attempt to alert the operators.

6.2 RSA Algorithm Encrypted TCP/IP Communication

The second layer of communication security protects the TCP socket connection between the Reactor Control PLC (serving as the connection host) and the remote operator workstation (serving as the connection client). Transport Layer Security version 1.3 (TLS 1.3) secures the TCP communication between the operator and the remote reactor's I&C system [Rescorla 2018]. This protocol employs RSA Encryption [Rivest, Shamir, and Adleman 1978] to encrypt the communications between the host and client to prevent tampering with the communication. The Reactor Control PLC stores the private key generated by the RSA algorithm. When establishing communication, the operator terminal requests that the PLC establish secure connection. The PLC's communication subroutine checks the authentication credentials supplied by the remote workstation to ensure that connection request is from an authorized terminal.

The PLC then sets up an asymmetric cypher for encrypting the TCP data packets communicated between the two [Rescorla 2018]. The PLC sends a temporary copy of the public key to the operator workstation for encrypting its communications, which can only be decrypted with the secure private key held on the

PLC. Unencrypted data packets and the packets encrypted using a different cypher are rejected by the connection [Rescorla 2018].

This two layer scheme guards against the VSLLIM microreactor receiving unauthorized commands or the reactor operations signals from being monitored by a system other than the operator terminal. The RSA encrypted TCP/IP connection protects against the data packets being intercepted and studied by a hostile party. The AES encryption algorithm protects against the potential compromise of the authentication credentials of the remote operator. Thus, even if a hostile actor successfully steals or fakes the correct authentication credentials, without the locally stored AES key, the VSLLIM I&C system would automatically reject any sent commands and any received monitoring data would be unintelligible. Similarly, even if a copy of the symmetric AES key is maliciously acquired, the communications would remain secured by the RSA encrypted connection.

6.3 Exception Handling

Long distance network communication involves risk that data packets could be lost due to network failures, physical damage to cables, or hostile actions to block communications. If the expected TCP/IP data is lost or delayed the systems log the event for the operator and default to the last known legitimate data values received through the secure data connection. This protects against short term disruptions and enables the VSLLIM digital twin to continue to operate normally while implementing the remote human operator's last commands. Similarly, the GUI data display of the remote operator workstation is programmed to plot the most recent known values. This exception handling scheme ensures the smooth continuous operation of the different communication programs. An extended communication outage between the remote operator and VSLLIM I&C system would be logged and the plant placed in a safe operation state to allow an alternative communication route to be established.

7. Testing Results of Remote Control of VSLLIM Digital Twin

The developed VSLLIM Digital Twin Remote Control Testbed is initially demonstrated at the UNM campus with the computers communicating through the university's ethernet network. The performed testing involves having the operator stationed remotely control the VSLLIM digital twin model through a series of operation transients. The scenarios to be demonstrated include reactor startup to different thermal power levels both with fresh fuel at Beginning-of-Life (BOL) and with partially burned fuel at different burnup levels, operation transients actively commanding PLC to increase and decrease the reactor power level. Also presented are results of a remote-control demonstration of researchers at Purdue University controlling the startup of the VSLLIM digital twin at UNM-ISNPS using the developed VSLLIM Digital Twin Remote Control Testbed.

7.1. Simulated Startup of the VSLLIM Microreactor at BOL

The developed startup scenario for the VSLLIM microreactor involves bringing the reactor to its full nominal operating power in two phases (Fig. 7). The first phase brings the reactor to steady state operation at a power level of 1 MW_{th}. This phase establishes steady natural circulation of the in-vessel Na and allows for the remote operator and on-site diagnostics to perform system check out and verify the instruments' function before further increasing the reactor power level. The second phase involves

increasing the reactor power setpoint to the desired operating power commanding the controllers to smoothly bring the reactor to steady state operation at the specified power level.

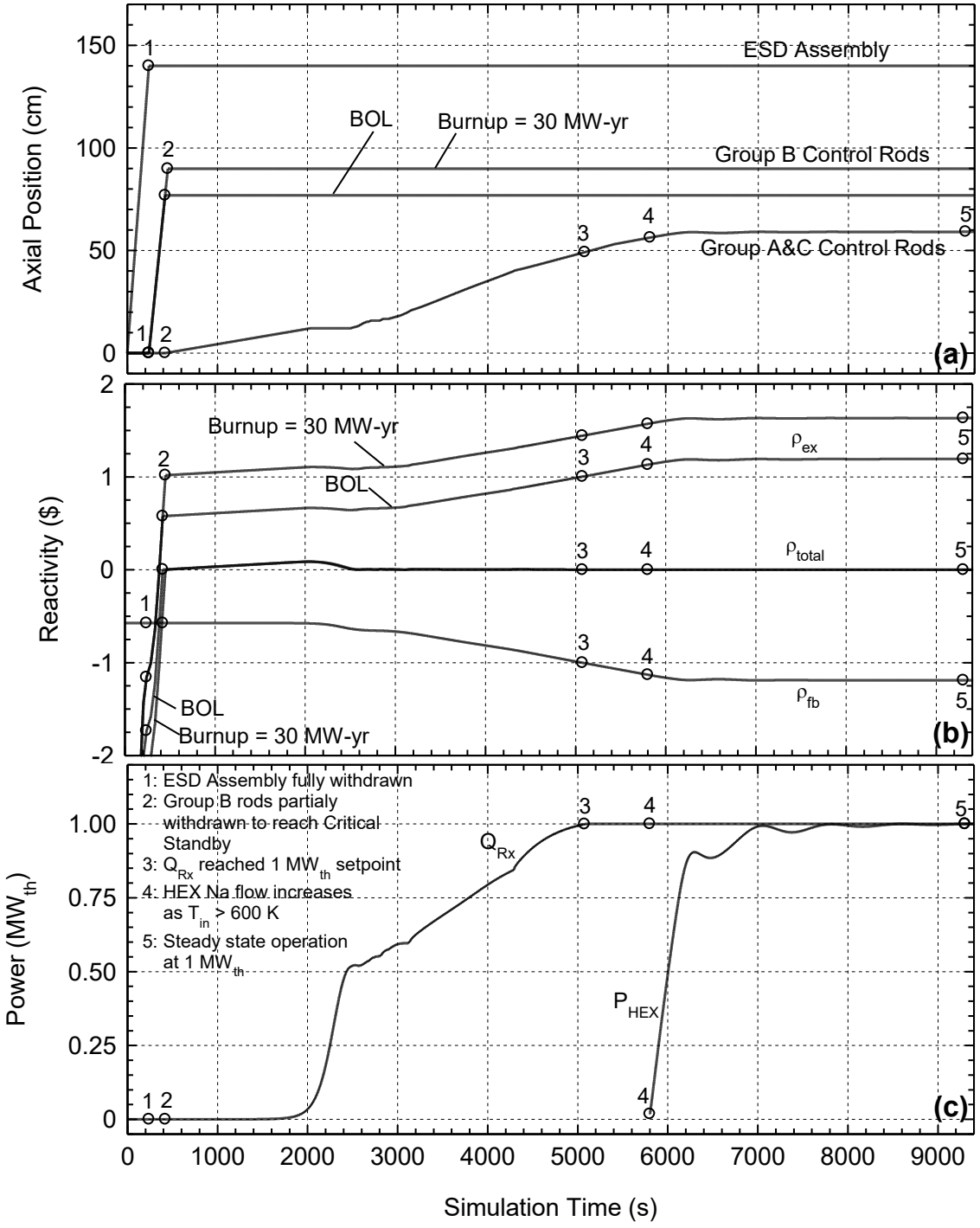

Fig. 16. Operation parameters of the remotely operated VSLLIM digital twin model during startup to a steady state power of 1.0 MW: (a) positions of the ESD assembly and the Group A, B, and C control rods, (b) total, external, and feedback reactivity, and (c) the reactor thermal power.

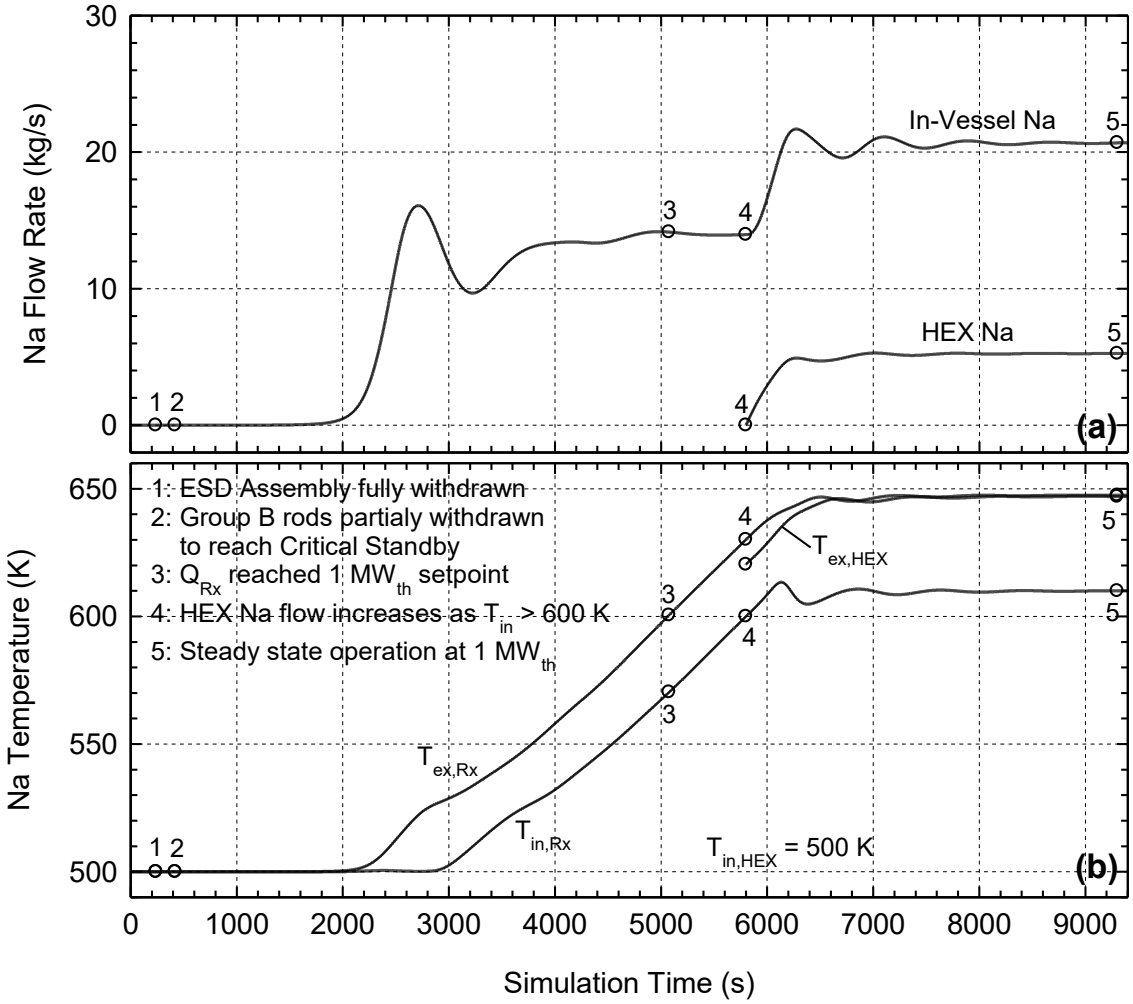

Fig. 17: Operation parameters of the remotely operated VSLLIM digital twin model during startup to a steady state power of 1.0 MW: (a) the mass flow rates of the in-vessel Na and the secondary Na in the helical coiled tubes of the Na/Na HEX, and (b) the sodium temperatures at the inlet and exit of the reactor core.

Prior to startup, electric heaters thaw the in-vessel Na within the VSLLIM microreactor bring it to a uniform temperature of 500 K. At time t = 0 the operator signals the Reactor Control PLC to fully withdraw the ESD center assembly from the reactor core over a period of 240 s (Point 1 in Fig 16a). After the withdrawal, the reactor is still subcritical (Fig. 16b). The operator then commands the Reactor Control PLC to bring the reactor to a critical state by axially withdrawing the Group B control rods (Point 2 in Fig. 16b).

Once the operator confirms that the reactor has reached criticality, they send a command for the PLC to simultaneously withdraw the Group A and C control rods to bring the reactor to the specified setpoint power, P_{SP} = 1 MW_{th}. The PLC initially withdraws the Group A and C rods at a constant rate of 0.75 mm/s until the reactor power reaches a steady value of 100 kW_{th}. Beyond this point, the trained SAC-FNN algorithm determines the withdrawal rates of the Group A and C control rods to increase the reactor thermal power to the setpoint P_{SP} = 1 MW_{th}.

The Reactor Control PLC acts to ensure a smooth rise of both the reactor power and the exit temperature of the in-vessel liquid Na from the reactor core (Figs. 16c and 17b). When the power reaches 1 MW_{th} the PLC maintains the reactor power constant (Fig. 16c) while the temperature of the in-vessel sodium increases (Fig. 17b). When the reactor inlet temperature exceeds a temperature of 600 K the HEX PLC begins increasing the flow rate of the secondary loop sodium in the helically coiled tubes to remove the power generated by the reactor (Figs. 17a and b).

The PLC adjusts the flow rate of the secondary loop liquid sodium to maintain the inlet temperature of the in-vessel sodium into the reactor core, T_{in}, at 610 K (Figs. 17a and b). As shown in Fig. 16c, the VSLLIM reactor reaches steady state operation at a reactor thermal power of 1.0 MW_{th} at t = 9,300 s.

7.1.1 Simulated Startup of the VSLLIM Microreactor with Increased Fuel Burnup

The results in Figs. 16 and 17 also show the results of a reactor startup with an initial fuel burnup of 30 MW-yr, ~51% of the total operation life of the reactor at a power of 10 MW_{th} [El-Genk and Palamino ref]. This burnup level reduces the excess reactivity in the reactor by 57.4 ¢ compared to that BOL. The Reactor Control PLC must withdraw the Group B control rods further from the core to compensate for the reduced core excess reactivity to bring the reactor up to the Critical Standby condition (Figs. 16a and 16b). The critical position for the Group B control rods increases from 76.9 cm at BOL to 89.9 cm for burnup of 30 MW-yr (Fig. 16a). This increased withdrawal distance only increases the Group B rod withdrawal time by ~20 s. After this small delay in the startup sequence relative to that for the core with fresh fuel at BOL, the startup sequence proceeds in the same manner as that described above in Section 7.1 (Figs. 16 and 17).

7.2. Simulated Startup of the VSLLIM Microreactor to Different Power Setpoints

The SAC-FNN algorithms were trained to perform the startup scenario from 0.5 to 1.0 MW_{th}. The remote and autonomous control system is evaluated to determine the performance when commanded to other power setpoints. Figs. 18a-d compare the calculated changes in the thermal power of the reactor controlled by PLC with the trained case Q model 53 SAC-FNN algorithm of 3 layers and 256 neurons per layer in four simulated startup transients. They begin from an initial reactor power setpoint $P_{SP,1}$ = 1.0 MW_{th} and continue to final power setpoints, $P_{SP,2}$, of 10.0 MW_{th}, 7.5 MW_{th}, 5.0 MW_{th}, and 2.0 MW_{th}, respectively. For $P_{SP,2}$ = 10.0 MW_{th} the PLC with the trained SAC-FNN algorithm withdraws Group A and C control rods to increase the VSLLIM microreactor power during the simulated startup transient. During the first ~11,400 s of the simulated startup transient the reactor thermal power is close to that calculated for the reactor controlled by the PLC with PD controller (Fig. 18a). Beyond such time, and while approaching $P_{SP,2}$ = 10.0 MW_{th}, the predicted rate of displacement of the control rods of Group A and C in the reactor core is 1.3% lower than the value determined by the PD controller.

In the simulated startup transients, the PLC with the trained SAC-FNN algorithm smoothly displaces the group A and C control rods in the reactor core (Figs. 18a and b). However, the predicted final reactor power by the PLC with the trained Case Q SAC-FNN algorithm is 2.8% above the target of 7.5 MW_{th} (Fig. 18b). In the simulated startup transients of the VSLLIM microreactor to $P_{SP,2}$ = 5.0 MW_{th}, the predicted final reactor power is ~ 2.5% higher than the target value (Fig. 18c). For the lowest power setpoint of $P_{SP,2}$ = 2.0 MW_{th}, the prediction of the PLC with the trained SAC-FNN algorithm matches the

final target power to within 0.1% (Fig. 18d). It is worth noting that the trained algorithms do not display consistent bias to over or underpredict the final reactor power.

Even though the SAC-FNN algorithms in this work are trained for a single target startup scenario of increasing the reactor power from 0.5 to 10.0 MW_{th}, the reactor control PLC performs well for lower $P_{SP,2}$ values. In conclusion, the PLC with the trained SAC-FNN algorithms performs well. The predicted displacements of the Group A and C control rods in the core of the VSLLIM microreactor during the simulated startup transients are comparable to those determined by the PLC with PD controller used to generate the training data for the SAC-FNN algorithms.

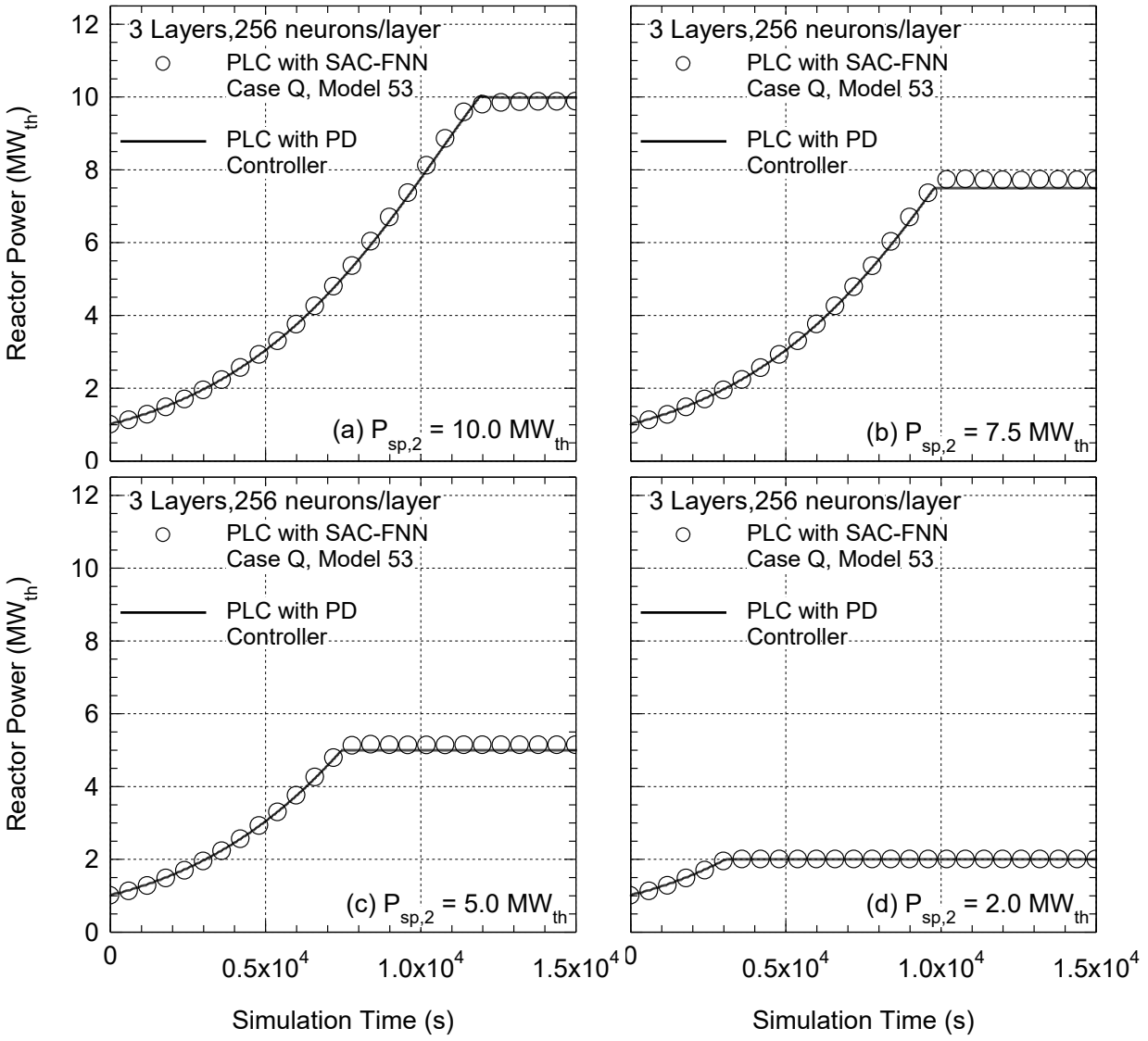

Fig. 18. Comparison of predicted reactor thermal power during a simulated startup of the VSLLIM microreactor by the Reactor Control PLC with the trained SAC-FNN algorithm in Case Q with 3 layers and 256 neurons per layer to those calculated in the simulated startup using the PLC with PD controller for target reactor power setpoints, $P_{SP,2}$, of: (a) 10.0 $MW_{th,}$ (b) 7.5 $MW_{th,}$ (c) 5.0 $MW_{th,}$ and (d) 2.0 MW_{th}.

7.3. Remote Control Demonstration between Purdue University and the University of New Mexico

The research teams at UNM-ISNPS and Purdue University conducted a demonstration on 29 October 2025. This included the secure remote control of the VSLLIM digital twin. Purdue's graduate students Zachery Dahm and Konstantinos Vasili served as the remote operators in the demonstration. UNM-ISNPS provided them with a user guide on the setup and operation of the VSLLIM remote control system. The demonstration began at 8:05 am MDT when the Purdue team logged into the computer running the remote-control console (Fig. 12). At 8:06 am MDT the VSLLIM digital twin Simulink model, LOBO NCS platform program, and PLCs were started by the team at UNM-ISNPS. The PLC was configured for the test with the case K model 26 trained SAC-FNN algorithm with 256 neurons per hidden layer [El-Genk, Schriener, and Shaheen 2025]. The Purdue graduate student researchers followed the instructions in the UNM-ISNPS provided user guide to start up the remote terminal program and GUI. The Purdue team successfully started the GUI as well as established a secure connection to the reactor control PLC at 8:16 am MDT.

The Purdue team began the startup procedure for the VSLLIM digital twin by sending the command to the PLC to withdraw the ESD assembly at 8:18 am MDT. The PLC sent a signal to the digital twin Simulink model to withdraw the assembly at a constant rate of 0.583 cm/s over a period of 240 s (Fig. 19a). Once they confirmed that the ESD assembly had been fully withdrawn from the core (Point 1 in Figs. 19a-d), the Purdue team sent the command to the PLC to bring the VSLLIM digital twin to zero power critical state at 8:22 am MDT. The PLC implemented this command by sending a signal to the Simulink model to withdraw the Group B control rods slowly at a rate of 0.428 cm/s (Fig. 19a).

This process continued until the PLC determined that the monitored value of the total reactivity from the VSLLIM digital twin model reaches critical condition (0$) and the withdraw of the Group B rods is halted (Point 2 in Fig. 19a-d). The Purdue team plotted the reactivity value using the real time plotting feature of the GUI and confirmed that the reactor had reached a critical state at 8:27 am MDT. Once they had sent the signal to the PLC that they had confirmed that the reactor was at the zero-power critical state, the Purdue team increased the reactor power setpoint to a value of 1 MW_{th} at time 1,294 s in the simulation.

The PLC adjusts the withdrawal rate for the Group A&C control rods to insert external reactivity to increase the reactor power (Fig. 19a). As the reactor power increases, the heat generated increases the temperature of the core and the in-vessel sodium (Figs. 19b and c). The flow to the Na-Na HEX is kept is kept to zero during this heat up period (Figs. 19d). Natural circulation of the in-vessel Na begins when a driving pressure develops between the lower density of hotter sodium in the core and exiting into the chimney and the higher density, colder sodium in the annular downcomer (Figs. 19c and d).

When the reactor power reaches the setpoint value of 1 MW_{th} at time t = 5,760 s the PLC continues to adjust the axial position of the Group A&C control rods to maintain the power constant while the in-vessel temperatures continue to increase (Figs. 19a). At time t = 6,592 s into the simulated transient the reactor inlet temperature exceeds 600 K and the HEX PLC begins increasing the flow rate of the secondary Na through the Na-Na HEX (Figs. 19c and d). During the approach to steady state the PLC with trained SAC-FNN algorithm overshoots the setpoint, exceeding 1 MW_{th} for several periods (Fig. 19a).

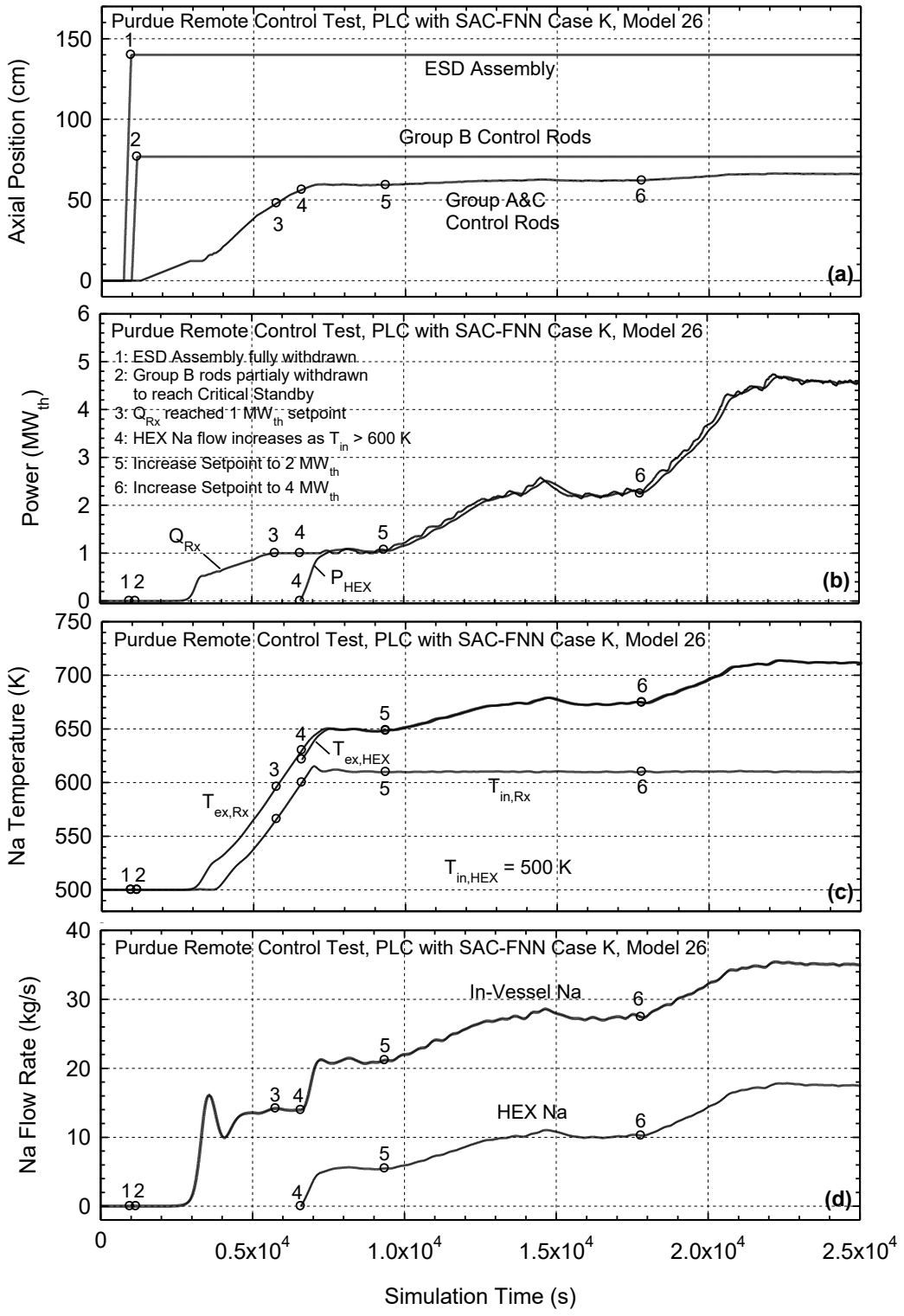

Fig. 19. Operation parameters of the remotely operated VSLLIM digital twin model operated by Purdue University: (a) positions of the ESD assembly and the Group A, B, and C control rods, (b) the reactor thermal power, (c) the mass flow rates of the in-vessel Na and the secondary Na in the helical coiled tubes of the Na/Na HEX, and (d) the sodium temperatures at the inlet and exit of the reactor core.

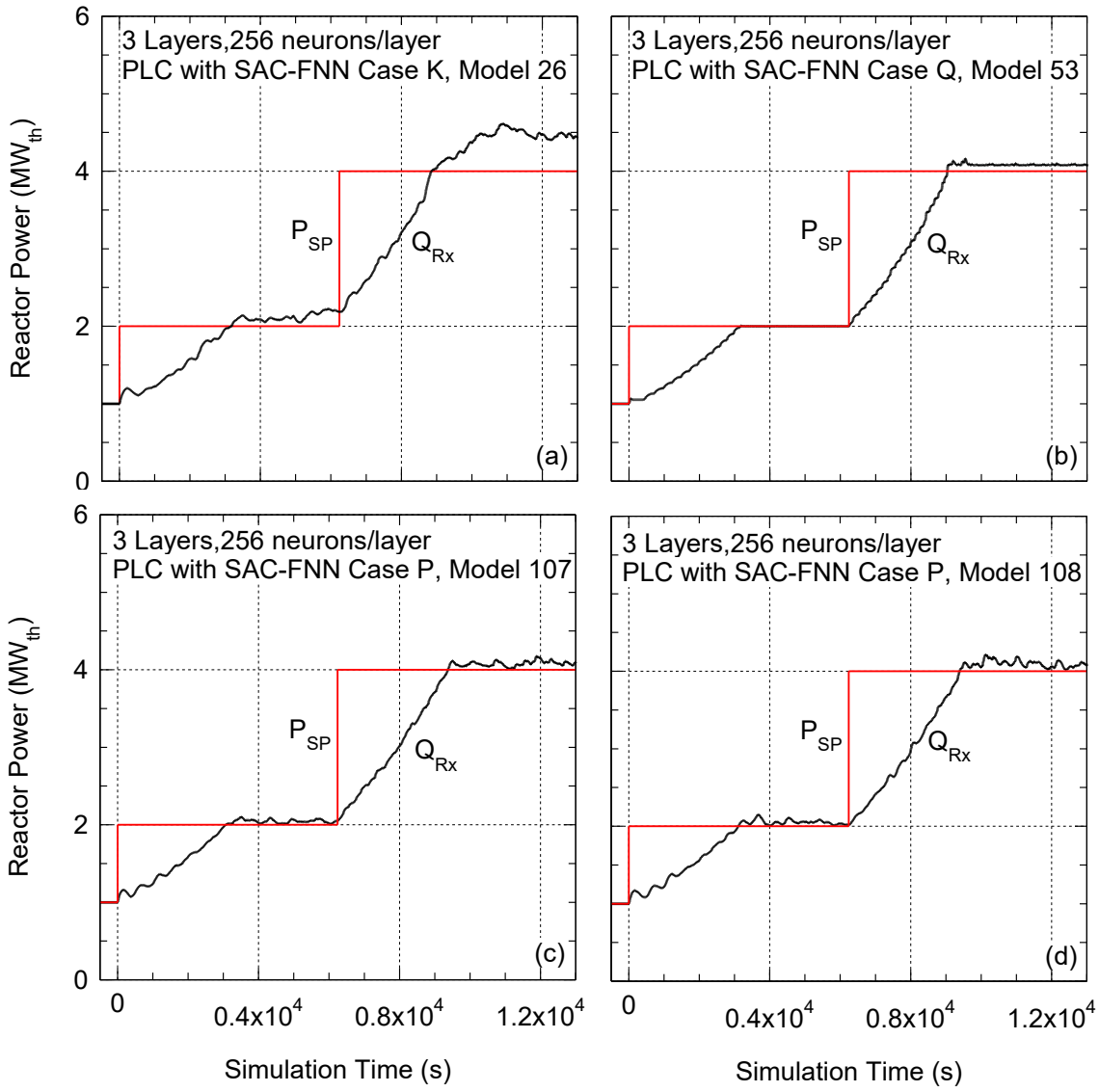

Fig. 20. Comparison of predicted reactor thermal power for remotely operated VSLLIM digital twin controlled by the Reactor Control PLC with the trained SAC-FNN algorithms with 3 layers, 256 neurons/layer of: (a) Case K Model 26, (b) Case Q Model 53, (c) Case P Model 107, and (d) Case P Model 108.

During testing it was found that the remote desktop software using the single session automatically generated passcodes which were logging the Purdue team out from the remote-control console computer. This resulted in a delay for the Purdue team in checking whether the system had reached steady state operation at the initial setpoint of 1 MW_{th}. The UNM-ISNPS team configured the remote program with a fixed user specified passcode which resolved the issue, allowing the Purdue team to reconnect at 10:29 am MDT. The Purdue team monitored the plant's state before deciding to increase the power setpoint to a value of 2 MW_{th} at 10:42 am MDT at time 9,354 s in the simulation. The PLC then continues to withdraw the Group A&C control rods to increase the reactor power. The used SAC-FNN algorithm overshoots the operator specified reactor power setpoint, with the power reaching up to 2.58 MW_{th} before decreasing

down to ~2.2 MW_{th} (Figs. 19a). The Purdue operators subsequently increased the power setpoint to 4 MW_{th} at time 17,786.5 s in the simulation. The PLC again overshot the power setpoint and reached a final reactor power of ~4.5 MW_{th}.

The observed overshooting of the reactor power by the PLC with trained SAC-FNN was investigated at UNM-ISNPS by repeating the startup scenario of increasing the reactor power in steps from 1 MW_{th} up to 2 and 4 MW_{th} using the four trained SAC-FNN algorithms with 3 layers and 256 neurons/layer (Fig. 20a-d). The results show that the control rod movement determined by the PLC with case K model 26 SAC-FNN results in the largest overshoot in the reactor power for the 2 MW_{th} and 4 MW_{th} power setpoints, reaching powers of ~2.2 and ~4.4 MW_{th} (Fig. 20a). The PLC with case Q model 53 SAC-FNN displays the best performance of the four trained algorithms, with the controller adjusting the control rod positions in a manner which produces the smallest power overshoot and oscillations during the simulated transient (Fig. 20b). The PLC with trained algorithm exactly matches the 2 MW_{th} power setpoint and reaches a power of 4.06 MW_{th} for the 4 MW_{th} power setpoint. The tests with the PLC with the case p model 107 and 108 SAC-FNN algorithms show that the PLC adjusts the control rod positions to reach the same power levels at the test with the PLC with case Q model 53 algorithm (Fig. 20b), but with larger oscillations (Figs. 20c-d). These tests results show that the remote-control real-time performance of the trained ML algorithms differs for power setpoints lower than the 10 MW_{th} value used in the training cases. Additional training using target cases with other power levels could potentially improve the performance of the SAC-FNNs for real-time control for lower power setpoints.

8. Summary

The work on Technical Task 2 investigated training the controllers of the VSLLIM microreactor for remote operation during startup transients using the SAC-FNN algorithms and evaluated the performance for real-time control of the VSLLIM microreactor during simulated transients. The trained SAC-FNN algorithms are incorporated into a PLC program for real-time control of a digital twin model of the VSLLIM reactor. The developed physics-based MATLAB dynamic Simulink model represents that of the digital twin of the VSLLIM microreactor for both training the algorithm and real time testing using the PLC.

The performed ML training using the SAC-FNN algorithm resulted in a total of thirteen algorithms that are successful in completing the VSLLIM startup scenario. The trained SAC-FNN algorithms incorporated into the Reactor Control PLC perform well, displacing the control rods for a steady rise in the reactor power that matches that of the PLC with PD controller. Four of the trained SAC-FNN algorithms have FNNs with three layers with 256 neurons per layer, and nine have FNNs with three layers with 64 neurons per layer. Unlike the previous testing in Task 1 with the PLC with the trained SL-LSTM algorithms, those with the trained SAC-FNN algorithms demonstrated good real-time control of the VSLLIM microreactor. In the SAC-FNN algorithms the reward feedback for actions during training helps them to take corrective actions to adjust the reactor thermal powers to match target values during the simulated startup transients.

The predictions with thirteen trained SAC-FNN algorithms agree with the target displacement curves of the Group A and C control rods in the microreactor core of to within ±1.6%. The PLC with the nine trained SAC-FNN algorithms of 64 neurons per layer reaches 9.5% lower reactor power from the setpoint of 10.0 MW_{th}. The PLC with the four trained SAC-FNN algorithms of 256 neurons per layer displayed

superior performance. These reach final reactor power levels that are ~0.5% higher than the setpoint of 10.0 MW_{th}. These trained algorithms with larger numbers of neurons learn better during the simulated startup transients and the predictions closely match the target data. And these algorithms were used for the subsequent remote-control testing.

The PLC with trained SAC-FNN algorithms is then incorporated into a developed testing platform for the secure remote control of the VSLLIM microreactor. The remote-control testbed includes an operator terminal with a GUI on a large format display for monitoring and plotting the operation state variables for the reactor. The remote human operator communicates with the Reactor Control PLC which is coupled to the VSLLIM digital twin model using the LOBO NCS platform. The developed secure communication scheme uses a two-step encryption method to secure the data transmitted between the VSLLIM digital I&C system and the remote operator terminal. The system employs both symmetric encryptions using a 128-bit AES encryption key and asymmetric encryption of the TCP/IP packets using the RSA encryption key. This scheme ensures that the transmitted data remains unintelligible if a hostile actor breaks one of the two levels. It also ensures that false commands or monitoring data are rejected if they are not encrypted with both keys correctly.

Testing of the developed remote-control platform has demonstrated the ability of a human operator using the remote-control terminal to command the VSLLIM digital twin and the PLC in its digital I&C system at the University of New Mexico. This has been demonstrated using remote operators at UNM campus in Albuquerque, NM and with operators on the Perdue campus in West Lafayette, In. The remote human operators can monitor the reactor's state in real time and send command to the PLC with trained SAC-FNNs coupled to smoothly start up the real-time transient VSLLIM digital twin model. The results using the PLC and different trained SAC-FNNs of 3 layers and 256 neurons / layer determined that while the networks all show satisfactory performance for the power setpoint of 10 MW_{th} used in training the algorithms, some displayed inconsistent performance for lower power setpoints. The PLC with the case Q model 53 SAC-FNN displayed the best performance incorporated into the VSLLIM digital twin remote control testbed, with the PLC able to adjust the control rod positions to reach the reactor power setpoints from 1-10 MW_{th} to within 2.8%.

Acknowledgements

This work supported by a DOE Office of Nuclear Energy's Nuclear Energy University Programs award through a subaward from Purdue University to the University of New Mexico's Institute for Space and Nuclear Power Studies under contract DE-NE0009268.

References

M. Abadi. TensorFlow: A System for Large-Scale Machine Learning, In Proceedings of 12th USENIX Symposium on Operating Systems Design and Implementation (OSDI'16), Savannah, GA, USA, 2-4 November 2016.

V. Agarwal, Y. A. Ballout, J. C. Gehin, "Fission Battery Initiative: Research and Development Plan," INL/EXT-21-61275, Idaho National Laboratories, Idaho Falls, ID, 2021

J. Bae, J. M. Kim, S. J. Lee. Deep reinforcement learning for a multi-objective operation in a nuclear power plant, *Nuclear Engineering and Technology*, 2023, 55(9), 3277-3290; https://doi.org/10.1016/j.net.2023.06.009S. M. Cetiner, et al., "Supervisory Control System for Multi-Modular Advanced Reactors," ORNL/TM-2016/693, Oak Ridge National Laboratory, Oak Ridge, TN, 2016.

L. A. Bernard, D. D. Lanning, A. Ray. Digital Control of Power Transients in a Nuclear Reactor, *IEEE Transactions on Nuclear Science*, 1984, 31(1), 701-705.

F. Chollet. Keras, 2015; https://keras.io

M. S. El-Genk, R. Altamimi, T. M. Schriener. Pressurizer Dynamic Model and Emulated Programmable Logic Controllers for Nuclear Power Plants Cybersecurity Investigations, *Annals of Nuclear Energy*, 2021, 154, 108121; https://doi.org/10.1016/j.anucene.2020.108121.

M. S. El-Genk, L. M. Palomino. A Walk-Away Safe, Very Small, Long-LIfe, Modular (VSLLIM) Reactor for Portable and Stationary Power, *Annals of Nuclear Energy*, 2019, 129, 181-198.

M. S. El-Genk, T. M. Schriener, L. M. Palomino. Passive and Walk-Away Safe Small and Microreactors for Electricity Generation and Production of Process Heat for Industrial Uses, *Nuclear Engineering and Radiation Science*, 2021, 7(3), 031302.

M. S. El-Genk, T. M. Schriener, A. N. Shaheen. *Training and Testing Machine Learning Algorithms for VSLLIM Reactor Controller.* Institute for Space and Nuclear Power Studies Technical Report No. UNM-ISNPS-01-2024, The University of New Mexico, Albuquerque, NM, 2024.

M. S. El-Genk, T. M. Schriener, A. N. Shaheen. Machine-Learning Algorithms for Remote-Control and Autonomous Operation of the Very-Small, Long-Life, Modular (VSLLIM) Microreactor, *J. Nuclear Engineering*, 2025, 6(4), 54. Doi: 10.3390/jne6040054

M. S. El-Genk, T. M. Schriener. A Cybersecurity Platform for Simulating Transient Responses of Emulated Programmable Logic Controllers in Instrumentation and Control Systems for a PWR Plant, *Journal of Cyber Security Technology*, 2022, 6(1-2), 65-90; https://doi.org/10.1080/23742917.2022.2059323

M. S. El-Genk, J.-M. Tournier. A Point Kinetics Model and Dynamic Simulation of Next Generation Nuclear Reactor, *J. Progress in Nuclear Energy*, 2016, 92, 91-103.

T. Goorley. *MCNP6.1.1-Beta Release Notes*, LA-UR-14-24680, Los Alamos National Laboratory, Los Alamos, New Mexico, USA 2014.

L. Hathaway, "National policy on the use of the advanced encryption standard (AES) to protect national security systems and national security information," National Security Agency, 23, pp. 149-171, 2003.

C. Li, A. Raghunathan, and N.K. Jha, "An architecture for secure software defined radio." IEEE Communications Surveys & Tutorials, **12**(4), pp. 531-550, 2010.

National Institute for Standards and Technology, Advanced Encryption Standard (AES), Federal Information Processing Standards Publication 197, Information Technology Laboratory National Institute of Standards and Technology Gaithersburg, MD, 2001.

E. Rescorla, "The Transport Layer Security (TLS) Protocol Version 1.3." Internet Engineering Task Force TLS workgroup, RFC 8446, 2018. doi:10.17487/RFC8446

R. Rivest, A. Shamir, L. Adleman, "A Method for Obtaining Digital Signatures and Public-Key Cryptosystems," Communications of the ACM, **21**(2), pp. 120–126, 1978.

T. M. Schriener, M. S. El-Genk. Simulated False Data Injection Attacks on Emulated and Hardware Programmable Logic Controllers of the Pressurizer in a Representative Pressurized Water Reactor Plant, *Journal of Cyber Security Technology*, 2022, 6(4), 216-241; https://doi.org/10.1080/23742917.2022.2123191

M. Serrano De Caro. *Irradiation Embrittlement in Alloy HT-9,* LA-UR-12-24334, Los Alamos National Laboratory, Los Alamos, NM, USA, 2012.

S. S. Sutton, A. G. Barto, *Reinforcement Learning, 2nd ed.*, MIT Press, Cambridge, MA, USA, 2018.

C. Tang, et al. Deep Learning in Nuclear Industry: A Survey, *Big Data Mining and Analytics*, 2022, 5(2), 140-160; DOI: 10.26599/BDMA.2021.9020027

The Mathworks. MATLAB version 2020b, 2022; www.matlab.com